Journal of *Marine Science and Engineering*

MDPI

Article

Functional Histology and Ultrastructure of the Digestive Tract in Two Species of Chitons (Mollusca, Polyplacophora)

Alexandre Lobo-da-Cunha [1,2,*], Ângela Alves [1,3], Elsa Oliveira [1,3] and Gonçalo Calado [4,5]

[1] Department of Microscopy, Institute of Biomedical Sciences Abel Salazar (ICBAS), University of Porto, Rua Jorge Viterbo Ferreira 228, 4050-313 Porto, Portugal; aralves@icbas.up.pt (Â.A.); emoliveira@icbas.up.pt (E.O.)
[2] Interdisciplinary Centre of Marine and Environmental Research (CIIMAR), 4450-208 Matosinhos, Portugal
[3] Multidisciplinary Unit for Biomedical Research (UMIB), ICBAS, University of Porto, 4050-313 Porto, Portugal
[4] Department of Life Sciences, Lusófona University, Campo Grande 376, 1749-024 Lisbon, Portugal; goncalo.calado@ulusofona.pt
[5] MARE—Marine and Environmental Sciences Centre, NOVA School of Science and Technology (FCT NOVA), Campus de Caparica, 2829-516 Caparica, Portugal
* Correspondence: alcunha@icbas.up.pt

Abstract: To continue the investigation on the digestive system of polyplacophoran molluscs, a histological and ultrastructural study of the oesophagus, stomach and intestine of *Chaetopleura angulata* and *Acanthochitona fascicularis* was carried out. Stomach content examination revealed an omnivorous diet. In both species the epithelium of the whole digestive tract consisted mostly of elongated absorptive cells with an apical border of microvilli. Cilia were also frequently present. Mitochondria and electron-dense lysosomes were the prominent organelles in the region above the nucleus. The basal region was characterised by an association of mitochondria, peroxisomes and lipid droplets. In general, glycogen deposits were also abundant in absorptive cells. The ultrastructural features indicate that the absorptive cells of the digestive tract epithelium are involved in endocytosis, intracellular digestion and storage of reserves. Histochemical techniques showed that the secretory cells of the digestive tract contained proteins and polysaccharides in their secretory vesicles. The secretory cells with vesicles of low electron density were classified as mucous cells, and the ones with electron-dense vesicles were designated basophilic cells due to their staining by basic dyes in light microscopy. Additionally, basal cells that seem to correspond to enteroendocrine cells containing oval electron-dense vesicles were found along the digestive tract epithelium of both species. The thin outer layer of the digestive tract wall consisted of muscle cells and nerves embedded in connective tissue.

Keywords: oesophagus; stomach; intestine; electron microscopy; histochemistry; Polyplacophora

Citation: Lobo-da-Cunha, A.; Alves, Â.; Oliveira, E.; Calado, G. Functional Histology and Ultrastructure of the Digestive Tract in Two Species of Chitons (Mollusca, Polyplacophora). *J. Mar. Sci. Eng.* **2022**, *10*, 160. https://doi.org/10.3390/jmse10020160

Academic Editor: Maria Gabriella Marin

Received: 20 December 2021
Accepted: 24 January 2022
Published: 26 January 2022

1. Introduction

Polyplacophorans, commonly known as chitons, are benthic marine molluscs characterized by their eight articulated dorsal shell plates surrounded by a flexible marginal girdle, which allows them to curl into a ball. This class of molluscs comprises approximately a thousand extant species, many of them living on rocky shores and others in deeper ocean floors [1–4]. The digestive system of chitons was described in classical articles [5], but very few studies were specifically dedicated to this subject in the last decades [6–9]. Moreover, the ultrastructure of the digestive tract was not previously investigated in these molluscs.

Most chitons are grazers that scrape hard surfaces in order to collect the algae and invertebrates included in their diets [8,10–12]. Others are ambush predators [13] or feed on sunken wood [14]. The broad and long radula used for feeding contains numerous hard teeth mineralised with magnetite and hydroxyapatite. It is formed within the radular sac that can extend back from the buccal cavity to approximately one third of the animal length [1,15]. Beneath the radular sac lies the subradular sac with a mucus-secreting epithelium. A bilobed subradular organ located dorsally near the distal end of the subradular

sac is lined by an epithelium mainly formed by cells with an apical microvillous border, containing electron-dense vesicles in the cytoplasm. Ciliated cells and some mucous cells are also present, and the dense innervation at the base of the epithelium suggests that the subradular organ has a chemosensory function [16].

Among chitons, a pair of small glands that have been called salivary glands are formed by large mucous cells interspersed with smaller wedge-shaped cells, but they were never studied by electron microscopy. In *Acanthochitona crinita*, *Cryptochiton stelleri* and *Stenoplax magdalenensis* these glands are branched and linked to the buccal cavity through very short ducts. Conversely, in *Lepidochitona cinerea*, a small size species, they are a simple sac opening directly into dorso-lateral buccal pouches [5]. The oesophagus is relatively short and it is linked to two large pouches known as "sugar glands" as they contain polysaccharide digesting enzymes [17]. These glands that were recently investigated by light and electron microscopy contain secretory cells and absorptive cells with many lysosomes [9]. The stomach of chitons is large and the gastric epithelium is formed by ciliated and non-ciliated supporting cells and secretory cells. The stomach is surrounded by branches of the digestive gland that is connected to the stomach by ducts [5,6]. Departing from the stomach, the long intestine is coiled around the digestive gland. A valve separating the anterior from the posterior intestine was reported in several species and the intestine ends in a short rectum with the anus located at the posterior end of the ventral surface of the animal [5,6,18]. However, despite some anatomical and histological descriptions, much remains to be known about the digestive tract of these marine molluscs. Thus, to continue the investigation on the digestive system of polyplacophorans, the oesophagus, stomach and intestine of *Chaetopleura angulata* (Spengler, 1797) and *Acanthochitona fascicularis* (Linnaeus, 1767) were investigated by light and transmission electron microscopy. Stomach content was also analysed to obtain some information about the diet of these species.

2. Materials and Methods

2.1. Collection Site, Digestive Tract Content and Measurements

Specimens of *Achantochitona fascicularis*, 3.0–4.5 cm in length, and *Chaetopleura angulata*, approximately 6 cm in length, were collected intertidally on Caldeira de Troia beach (38.49° N, 8.89° W) at the mouth of the Sado estuary (Portugal) (Figure S1). For histology and ultrastructure, live specimens were transported to the laboratory in a container with local water. Five specimens of each species were used for histological sections and small segments of the digestive tract, also obtained from 5 specimens, were processed for semithin and ultrathin sections. For analysis of stomach content, 3 specimens of each species were dissected at the collection site and their digestive tract was immediately preserved in 10% formalin made with seawater. In the laboratory the stomach content was analyzed and photographed under a stereomicroscope and further observations were made with a light microscope. For length determination, the intestine was carefully removed from unfixed specimens and measured with a ruler avoiding stretching. Several unfixed transverse sections of the anterior and posterior intestine without fecal material in the lumen were photographed under a stereomicroscope and the images were used to evaluate the intestine diameter. Other measurements were made on photomicrographs of semithin or ultrathin sections.

2.2. Tissue Processing for Light and Transmission Electron Microscopy

For histological sections, isolated oesophagus, whole stomachs and several segments of anterior and posterior intestine were fixed for 24 h with Bouin's solution, dehydrated in a graded series of ethanol and embedded in paraffin. Additionally, the same procedure was applied to the entire visceral mass of other specimens. Sections with a thickness of 5 µm were stained with Masson's trichrome, dehydrated, cleared with xylene and mounted with Coverquick 2000 medium.

For semithin and ultrathin sections, several samples of oesophagus, stomach, anterior and posterior intestine were fixed for 2 h at 4 °C in 2.5% glutaraldehyde and 4% formalde-

hyde (obtained from hydrolysis of para-formaldehyde), diluted with 0.4 M cacodylate buffer pH 7.4 (final buffer concentration 0.28 M). After washing in buffer, samples were postfixed with 2% osmium tetroxide buffered with cacodylate, dehydrated in increasing concentrations of ethanol and embedded in epoxy resin (Fluka). For light microscopy observations semithin sections with a thickness of 2 µm were stained with methylene blue and azure II. Semithin sections were also used for histochemical stainings. Ultrathin sections were stained with uranyl acetate for 20 min and lead citrate for 10 min. To enhance glycogen staining, some ultrathin sections were stained with 2% uranyl acetate for 10 min after 10 min treatment with a solution of tannic acid at 5% [19]. Ultrathin sections were observed in a JEOL 100CXII transmission electron microscope.

2.3. Histochemistry

Histological sections of Bouin-fixed samples with a thickness of 5 µm were stained by the periodic acid–Schiff (PAS) reaction for polysaccharide detection, Alcian blue staining at pH 1.0 for sulphated acid polysaccharides or Alcian blue at pH 2.5 for carboxylated acid polysaccharides. For PAS reaction sections were oxidised with 1% periodic acid for 10 min, washed with water, and stained with Schiff reagent for 20 min. For Alcian blue staining sections were stained for 30 min in 1% Alcian blue in a HCl solution with pH 1.0 or in acetic acid for pH 2.5 [20]. Some sections were stained by both PAS reaction and Alcian blue. Additionally, PAS reaction, Alcian blue staining, tetrazonium coupling reaction for protein detection and Sudan black staining for lipids were applied to 2 µm thick semithin sections of epoxy embedded samples. For PAS reaction, semithin sections with resin were treated with 1% periodic acid for 10 min, washed with water, and stained with Schiff reagent for 20 min. For Alcian blue staining, resin was removed using an alcoholic solution of sodium ethoxide, prepared by dissolving sodium hydroxide to saturation in absolute ethanol [21]. Subsequently, sections were thoroughly washed in absolute ethanol and water, and stained for 30 min in 1% Alcian blue solution in acetic acid, for pH 2.5, or in a HCl solution with pH 1.0. For the tetrazonium reaction, semithin sections with resin were treated with a freshly-prepared 0.2% solution of fast blue salt B in 0.1 M veronal-acetate buffer pH 9.2, for 10 min. After washing, sections were treated for 15 min with a saturated solution of β-naphthol in 0.1 M veronal-acetate buffer pH 9.2. For Sudan black staining semithin sections with resin were treated for 10 min with a 0.02% H_2O_2 solution to remove osmium tetroxide. After washing in water, sections were stained for 5 min with a saturated solution of Sudan black in 70% ethanol and washed in 70% ethanol. After washing, semithin sections with resin were air dried before being mounted with Coverquick 2000 medium. Alcian blue stained semithin sections without resin were dehydrated and cleared with xylene before mounting.

2.4. Ultrastructural Detection of Arylsulphatase Activity

For detection of the lysosomal enzyme arylsulphatase, small fragments of stomach and intestine were fixed for 1 h at 4 °C in 2.5% glutaraldehyde and 4% formaldehyde (obtained from hydrolysis of para-formaldehyde), diluted in 0.4 M cacodylate buffer pH 7.4. After washing in buffer, samples were incubated during 45 min at 35 °C in medium containing 40 mM $BaCl_2$ and 25 mM p-nitrocatechol sulfate in 0.2 M acetate buffer pH 5.0 [22]. For control, some tissue fragments were incubated in medium without p-nitrocatechol sulfate. Post-fixation was carried out for 2 h at room temperature with 1% OsO_4 and 1.5% potassium ferrocyanide in cacodylate buffer. Ultrathin sections were observed without further staining.

3. Results

3.1. General Morphology and Content of the Digestive Tract

A short oesophagus with an average diameter of 1.4–1.5 mm in *Chaetopleura angulata* and 0.9–1.0 mm in *Acanthochitona fascicularis* linked the buccal cavity to stomach. The large stomach with a complex shape presented a constriction in which a portion of the digestive gland was lodged. The long intestine departed from the stomach and formed several

coils around the digestive gland (Figure 1A,B). In specimens of *C. angulata* approximately 6 cm long the total intestine length was 17.0–20.0 cm, being 7.0–10.5 cm in *A. fascicularis* specimens with a body length of 3.0–4.5 cm. Accordingly, in these species the intestine length/animal length ratio was in average 3.0 (SD 0.3) and 2.4 (SD 0.3), respectively. In *C. angulata* the diameter of the intestine was around 1.3–1.7 mm in the region close to the stomach and 0.8–1.2 mm for most of its length. In *A. fascicularis* a short constricted region with a length of 3.0–4.0 mm formed a valve separating the anterior from the posterior intestine (Figure 1A inset). In this last species, the anterior intestine corresponded to 20–25% of the total intestine length and had a diameter of 1.2–1.4 mm in the largest specimens that were observed, whereas in the posterior intestine the diameter was around 0.7–1.1 mm. In *C. angulata* a constricted region clearly separating the anterior from the posterior intestine was not observed, and in this case the first 3–4 cm of intestine (approximately 20% of the total length) were considered to correspond to the anterior intestine.

Figure 1. General view of the digestive system. (**A**) Stereomicroscope view of the digestive system of *A. fascicularis*. Inset, narrow segment (arrow) corresponding to the valve between the anterior (ai) and posterior intestine (pi). (**B**) Histological section of the digestive system of *C. angulata* stained by Masson's trichrome. dg—digestive gland, in—intestine, op—oesophageal pouches (sugar glands), st—stomach.

The analysis of the stomach content of *C. angulata* revealed remains of crustaceans, a few foraminiferans, diatoms and fragments of multicellular green and red algae

(Figure 2A–E). The stomach of *A. fascicularis* contained mainly fragments of multicellular green and red algae, diatoms and a few foraminiferans among unidentifiable debris (Figure 2F–I). However, small crustaceans or other invertebrates were not found in the digestive tract of *A. fascicularis*.

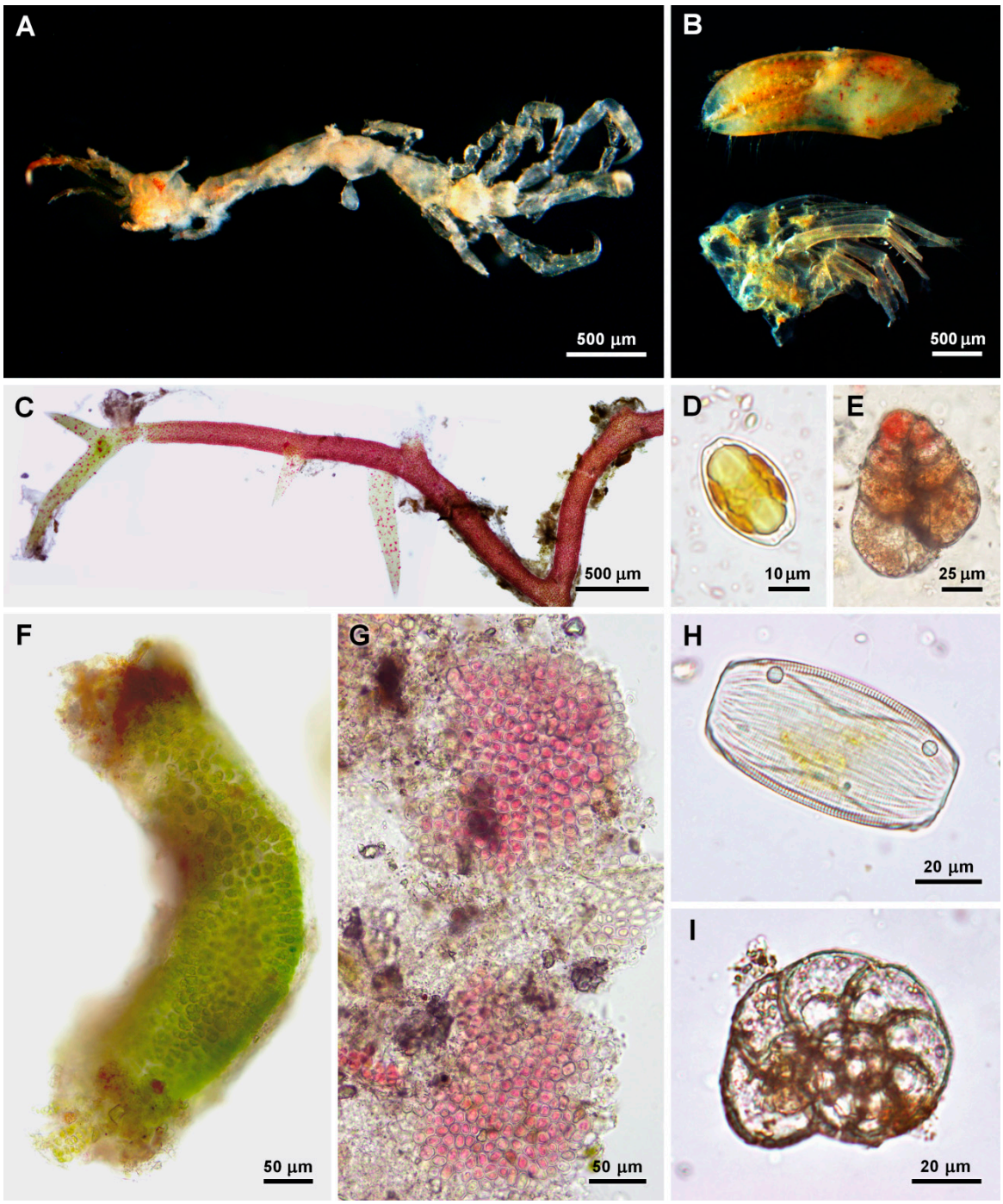

Figure 2. Digestive tract content. (**A**–**E**) A caprellid amphipod (**A**), fragments of other crustaceans (**B**), a piece of red algae (**C**), a diatom (**D**) and a foraminiferan (**E**) from the stomach of *C. angulata*. (**F**–**I**) Fragments of green (**F**) and red algae (**G**), a diatom frustule (**H**) and a foraminiferan (**I**) from the stomach of *A. fascicularis*.

3.2. Histology and Ultrastructure of the Oesophagus

The oesophagus had ridges created by large differences in epithelial thickness. The height of this epithelium was very variable, being around 25 µm at the thinner points between ridges and reaching about 200 µm in some ridges in transverse semithin sections of the oesophagus of both species. The outer layer of the oesophageal wall consisted of connective tissue, muscle cells and many nerves, usually with a thickness of 40–60 µm in *C. angulata* and 20–30 µm in *A. fascicularis* (Figure 3A–C). Light microscopy observations showed that the oesophageal epithelium consisted mostly of very thin and long absorptive cells with a microvilli border and cilia. In semithin sections stained by methylene blue and azure II, several blue stained bodies were detectable in the apical region of the absorptive cells. Osmiophilic lipid droplets were also noticeable in these cells (Figure 3D). The nuclei were elongated, several of them about 2.5 µm wide and 15 µm long, and in general were positioned in the central region of the cell.

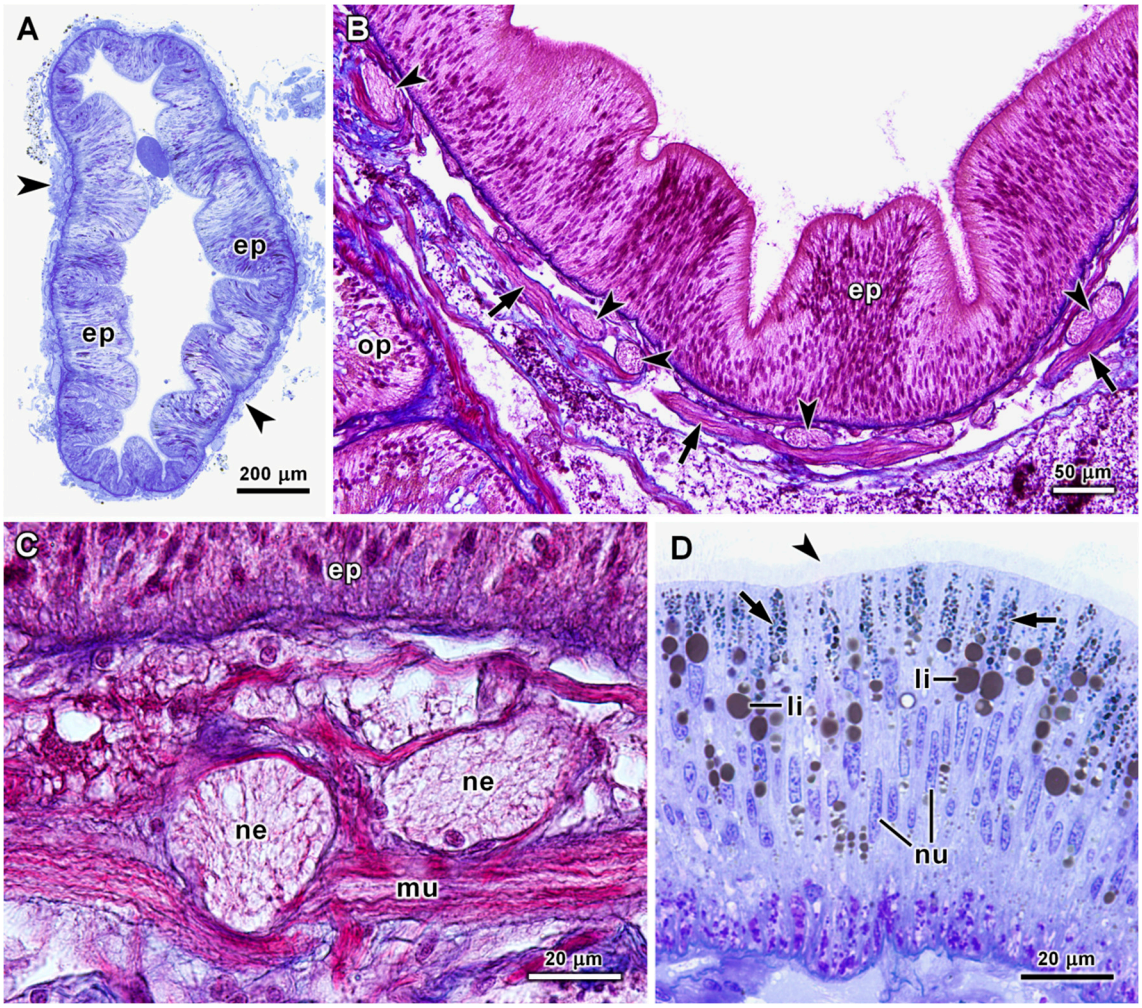

Figure 3. Histology of the oesophagus of *A. fascicularis* (**A**) and *C. angulata* (**B**–**D**). (**A**) Transverse semithin section of the oesophagus. The epithelium (ep) is surrounded by a layer of connective tissue with muscular cells and nerves (arrowheads). Methylene blue and azure II staining. (**B**) Several nerves (arrowheads) and muscle fibres (arrows) surround the oesophageal epithelium (ep). Masson's trichrome staining. (**C**) Higher magnification view of two nerves (ne) and muscle fibres (mu) below the oesophageal epithelium (ep). Masson's trichrome staining. (**D**) Absorptive cells with a microvilli border (arrowhead), inclusions in the apical region of the cytoplasm (arrows) and lipid droplets (li) in a semithin section of the oesophagus stained by methylene blue and azure II. nu—nuclei, op—oesophageal pouches (sugar glands).

Two types of secretory cells were identified in the oesophageal epithelium. In *A. fascicularis* the basophilic secretory vesicles of both cell types presented a dark blue colour in semithin sections stained by methylene blue and azure II. These secretory vesicles were also stained by tetrazonium and PAS reactions indicating a secretion rich in both proteins and polysaccharides (Figure 4A–E). However, in one secretory cell type the vesicles were significantly larger, most of them with a diameter of 1.0–2.5 µm in semithin sections, whereas in the other secretory cell type they seldom reached 0.9 µm (Table 1). Additionally, Alcian blue staining revealed the presence of acid polysaccharides only in the secretion of the cells with smaller vesicles (Figure 4F), which were designated as basophilic cells with small vesicles. For distinction, the secretory cells with larger vesicles were designated as basophilic cells with large vesicles (Table 1). In *C. angulata* oesophagus, in one cell type the cytoplasm above the nucleus was filled with a compact mass of secretory vesicles that stained purple-blue with methylene blue and azure II (Figure 4G). These secretory cells that were classified as mucous were stained by PAS reaction (Figure 4H) and Alcian blue at pH 1.0 and 2.5, but staining with the tetrazonium reaction was weaker (Table 1). The other type of secretory cells in *C. angulata* oesophagus was characterized by vesicles clearly separated from each other, reaching 3.0 µm in diameter in semithin sections. Nevertheless, some cells contained smaller secretory vesicles. These basophilic vesicles stained dark blue with methylene blue and azure II, and were strongly stained by PAS and tetrazonium reactions in semithin sections (Figure 4I), but were not stained by Alcian blue. At the bottom of the epithelium, basal cells were abundant with many small purple vesicles in semithin sections stained by methylene blue and azure II (Figure 4J), which were also stained by the tetrazonium coupling reaction (Table 1).

Table 1. Characterization of secretory cells of the digestive tract of *C. angulata* and *A. fascicularis*.

Organs	Species	Cell Types	Diameters of Secretory Vesicles (µm) [1]	PAS Reaction (Polysaccharides)	Alcian Blue pH 1.0 and 2.5 (Acid Polysaccharides)	Tetrazonium Reaction (Proteins)	Electron Density of Vesicles
Oesophagus	*C. angulata*	Basophilic	1.0–3.0	+ + +	–	+ + +	High
		Mucous	0.3–0.7	+ +	+ + +	+ +	Low
	A. fascicularis	Basophilic with small vesicles	0.4–0.9	+ + +	+ + +	+ +	High
		Basophilic with large vesicles	1.0–2.5	+ + +	–	+ + +	High
Stomach	*C. angulata*	Basophilic	0.4–0.8	+ + +	–	+ + +	High
	A. fascicularis	Basophilic	0.6–1.1	+ + +	–	+ + +	High
Intestine	*C. angulata*	Basophilic	0.4–0.8	+ + +	–	+ + +	High
		Mucous [2]	0.8–1.8	–	+ + +	–	Low or median
	A. fascicularis	Basophilic	0.5–1.5	+ + +	+ +	+ +	High
		Mucous [3]	(undetermined due to fusion)	+ + +	+ +	+	Low
	C. angulata	Basal cells (enteroendocrine)	0.4–1.0	–	–	+ + +	High
	A. fascicularis	Basal cells (enteroendocrine)	0.2–0.5	–	–	+ + +	High

Average stain intensity: – unstained; + weak; + + moderate; + + + strong; [1] Corresponding at least to 95% of the vesicle diameters in semithin or ultrathin sections; [2] In the valve between the anterior and posterior intestine, and in the posterior intestine; [3] In the valve between the anterior and posterior intestine.

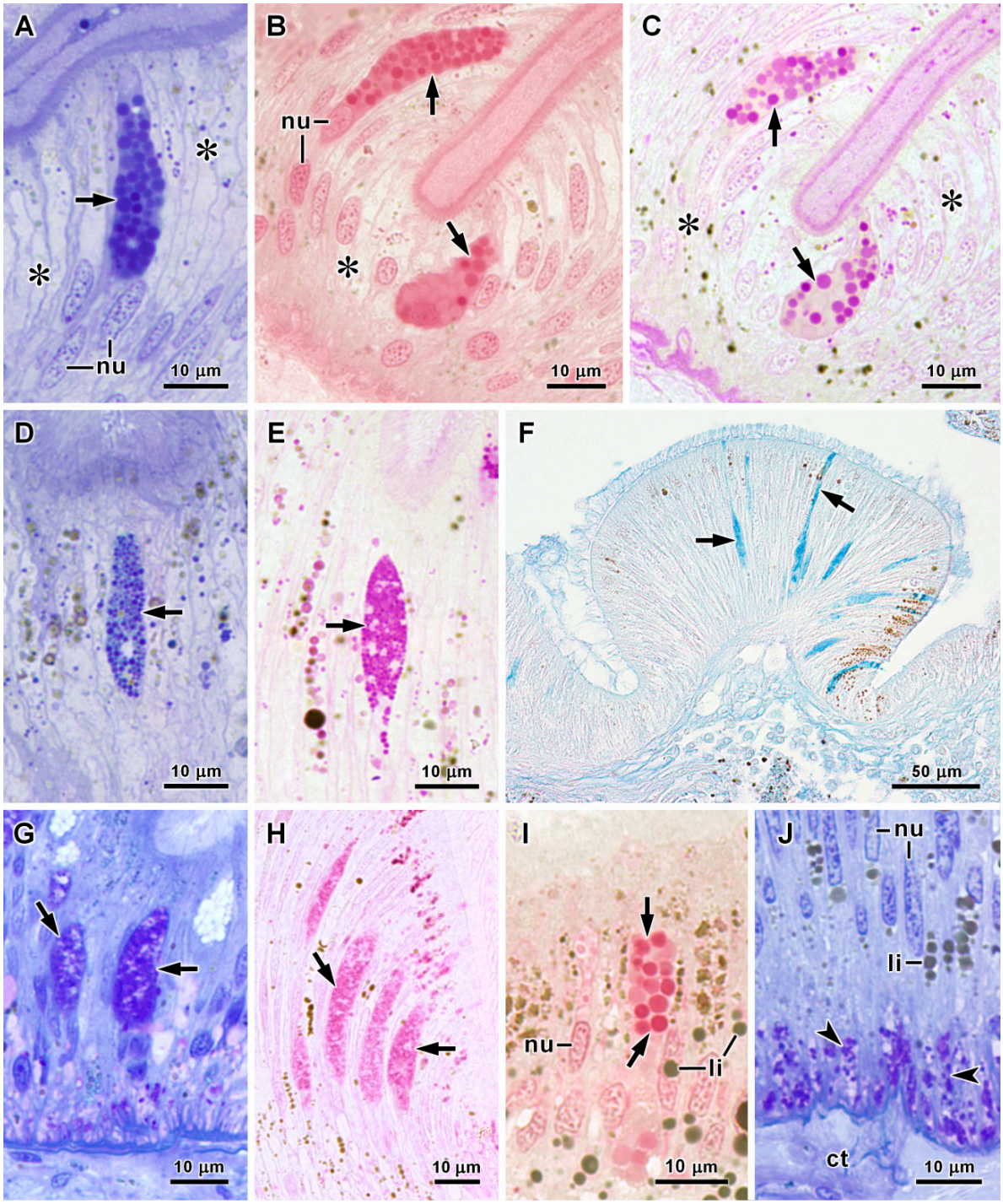

Figure 4. Oesophagus of *A. fascicularis* (**A**–**F**) and *C. angulata* (**G**–**J**), in semithin (**A**–**E**,**G**–**J**) and histological (**F**) sections. (**A**–**C**) Absorptive cells (asterisks) and basophilic cells with large secretory vesicles (arrows) in the oesophagus of *A. fascicularis* stained by methylene blue and azure II (**A**), tetrazonium coupling reaction for protein detection (**B**) and PAS reaction for polysaccharide detection (**C**). (**D**–**F**). Basophilic cells with small secretory vesicles (arrows) in the oesophagus of *A. fascicularis* stained by methylene blue and azure II (**D**), PAS reaction (**E**) and Alcian blue for acid polysaccharide detection (**F**). (**G**,**H**) Mucous cells (arrows) in the oesophagus of *C. angulata* stained by methylene blue and azure II (**G**) and PAS reaction (**H**). (**I**) Basophilic cell with large secretory vesicles (arrows) in the oesophagus of *C. angulata* stained by the tetrazonium coupling reaction. (**J**) Basal cells of the oesophagus with purple vesicles (arrowheads) in a section stained with methylene blue and azure II. ct—connective tissue, li—lipid droplets, nu—nuclei.

The absorptive ciliated cells of the oesophagus were ultrastructurally similar in both species. Several mitochondria, vesicles and some multivesicular bodies occurred in the most apical portion of the cytoplasm. In these cells, the electron-dense lysosomes were the prominent features in the cytoplasm above the elongated nucleus (Figure 5A). The vast majority of these lysosomes had diameters of 0.5–2.0 µm in ultrathin sections, and a few largest ones presented diameters up to 3.5 µm. These organelles correspond to the blue inclusions observed by light microscopy in semithin sections stained with methylene blue and azure II. Some mitochondria, lipid droplets, Golgi stacks and endoplasmic reticulum cisternae were present in the middle of these cells. Conversely, the most basal region was characterized by a large accumulation of mitochondria associated with peroxisomes and some lipid droplets (Figure 5B). Crystalline cores were absent in the peroxisomes that had diameters of 0.3–0.6 µm in ultrathin sections. Deep cell membrane invaginations were another feature of the basal region of absorptive cells. In the oesophagus of *C. angulata* the basophilic cells contained round electron-dense secretory vesicles and the flattened cisternae of rough endoplasmic reticulum filled a considerable part of the cytoplasm around the secretory vesicles (Figure 5C). The Golgi stack cisternae and associated vesicles contained electron-dense substances, although not so electron-dense as the mature secretory vesicles (Figure 5D). On the other hand, in mucous cells the secretory vesicles were closely aggregated and many had fused forming vacuoles of diverse sizes filling most of the cytoplasm. These vesicles had an electron-dense spot and filaments embedded in a matrix of lower electron density (Figure 5E). In these cells the cisternae of rough endoplasmic reticulum were dilated and the Golgi stacks cisternae had an electron-lucent content (Figure 5F). In *A. fascicularis* both types of secretory cells contained electron-dense vesicles, the difference residing in vesicle diameter as observed with the light microscope (Table 1). An additional difference was found in the rough endoplasmic reticulum of these cells. The ones with the smaller secretory vesicles contained dilated cisternae, whereas in the cells with larger vesicles the cisternae were mostly flattened (Figure 6A,B). In both species, basal cells with round and oval electron-dense vesicles in a clear cytoplasm were frequently found in ultrathin sections of the oesophageal epithelium. However, in average the vesicles of basal cells were larger in *C. angulata* (Table 1). The cytoplasmic extensions of these cells were intertwined with the basal region of the absorptive cells, but a few basal cells with a long apical process were also observed (Figure 6C,D). However, it was not possible to see if these apical processes reached the lumen of the oesophagus. The outer layer of the oesophageal wall included smooth muscle cells and many nerves containing several axons and some glial cells, embedded in the connective tissue matrix (Figure 6D).

3.3. Histology and Ultrastructure of the Stomach

The stomach epithelium was identical in both species, being mainly formed by elongated absorptive cells with a central nucleus (Figure 7A,B). Epithelial height measured in semithin sections ranged mostly from about 40 µm at the thinner points between ridges to near 100 µm in thicker ridges, without significant differences detect between the two species. A layer of connective tissue, muscle fibres and some nerves formed the outer layer of the stomach wall usually with a thickness of 15–25 µm in *C. angulata* (Figure 7A) and 5–15 µm in *A. fascicularis*. With the light microscope only one type of secretory cells could be recognized in this epithelium, looking similar in both species. Their basophilic secretory vesicles stained dark blue with methylene blue and azure II, and were also strongly stained by PAS and tetrazonium reactions, but were not stained by Alcian blue (Figure 7B–F) (Table 1). Additionally, the microvilli layer covering the absorptive cells was stained by the PAS reaction in *A. fascicularis* (Figure 7E). As in the oesophagus, basal cells were present in the epithelium and their vesicles were stained by the tetrazonium coupling reaction for protein detection (Figure 7G).

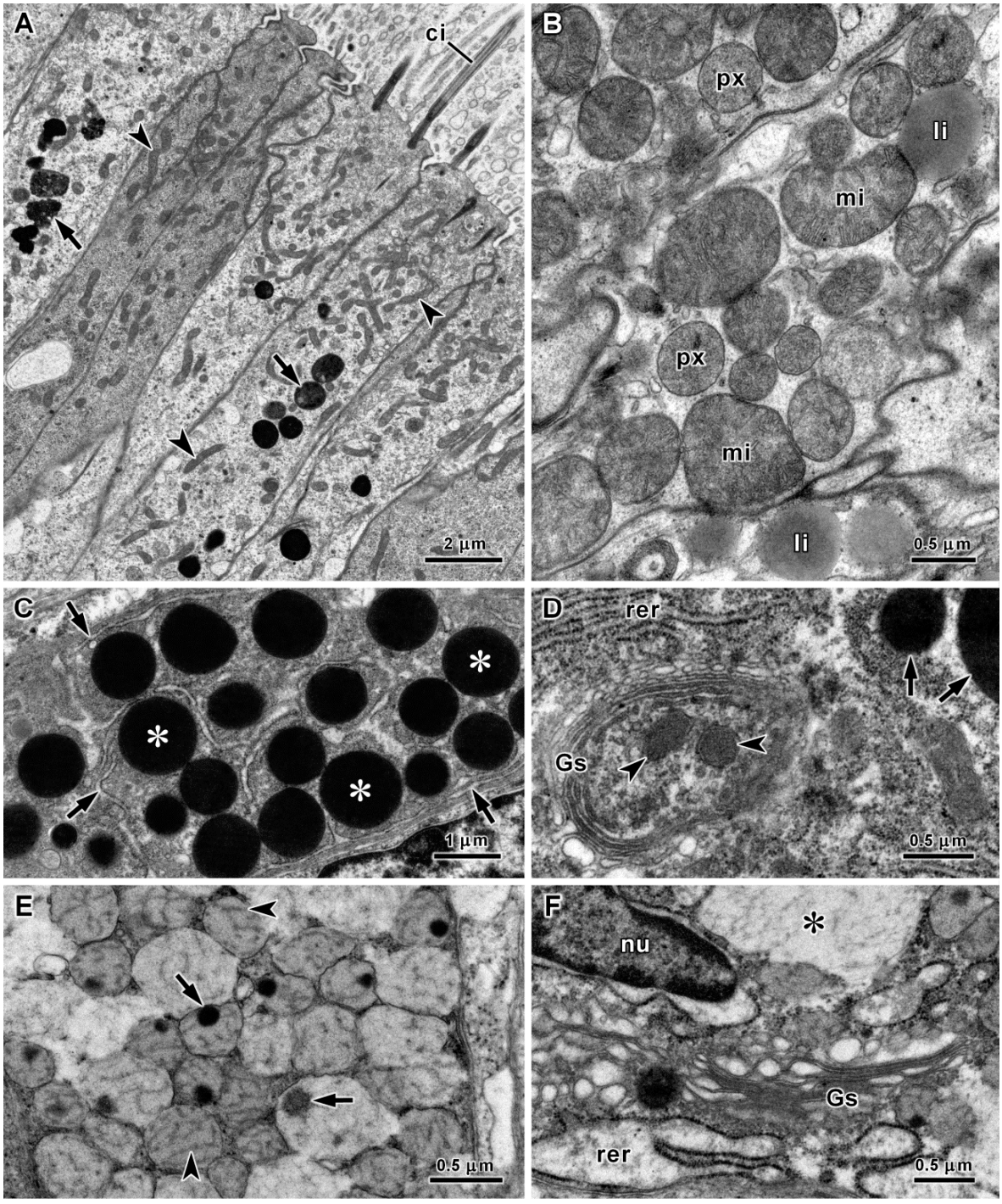

Figure 5. Ultrastructure of the oesophagus in *C. angulata* (**A**,**C**–**F**) and *A. fascicularis* (**B**). (**A**) Ciliated absorptive cells with several mitochondria (arrowheads) and lysosomes (arrows) in the apical cytoplasm. (**B**) Mitochondria (mi), peroxisomes (px) and lipid droplets (li) in the basal region of an absorptive cell. (**C**) Basophilic cell with electron-dense secretory vesicles (asterisks) and flattened cisternae of rough endoplasmic reticulum (arrows). (**D**) Golgi stack (Gs) and associated vesicles (arrowheads) with a content less electron-dense than the mature secretory vesicles (arrows) in a basophilic cell. (**E**) In mucus-secreting cells vesicles contained an electron-dense spot (arrows) and filaments (arrowheads). (**F**) Golgi stack (Gs) and dilated cisternae of rough endoplasmic reticulum (rer) in a mucus-secreting cell. Vesicle fusion created vacuoles with secretory products (asterisk). ci—cilium, nu—nucleus, rer—rough endoplasmic reticulum.

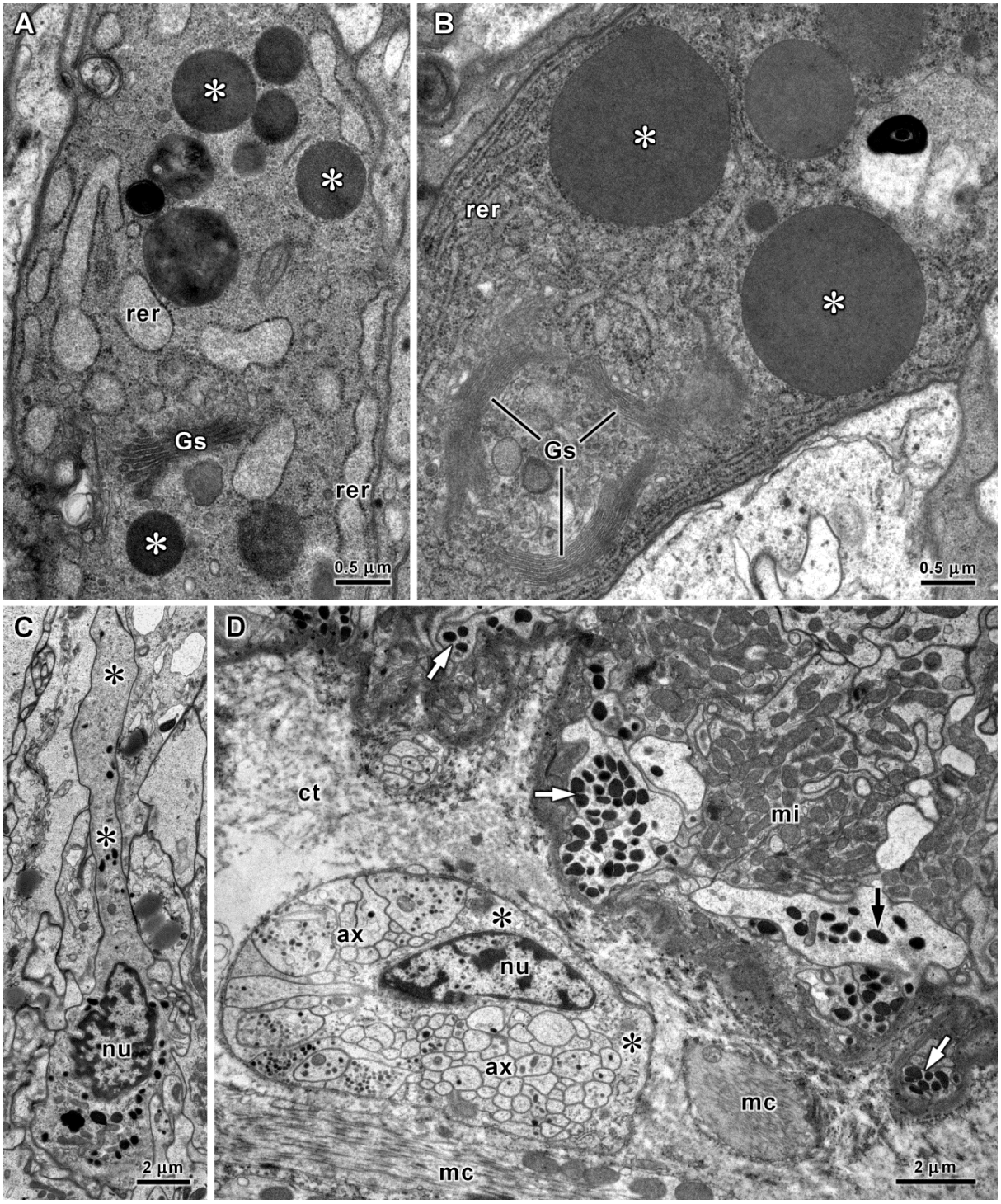

Figure 6. Ultrastructure of the oesophagus in *A. fascicularis*. (**A**) Basophilic cell with small electron-dense secretory vesicles (asterisks), dilated rough endoplasmic reticulum cisternae (rer) and a Golgi stack (Gs). (**B**) Basophilic cell with large electron-dense secretory vesicles (asterisks), flattened rough endoplasmic reticulum cisternae (rer) and Golgi stacks (Gs). (**C**) Basal cell with a long apical process (asterisks). (**D**) Basal region of the epithelium with basal cells containing electron-dense secretory vesicles (arrows). Many mitochondria (mi) are visible in the basal region of the absorptive cells. Muscle cells (mc) and a nerve section with several axons (ax) and a glial cell (asterisks) can be seen below the epithelium. ct—connective tissue matrix, nu—nuclei.

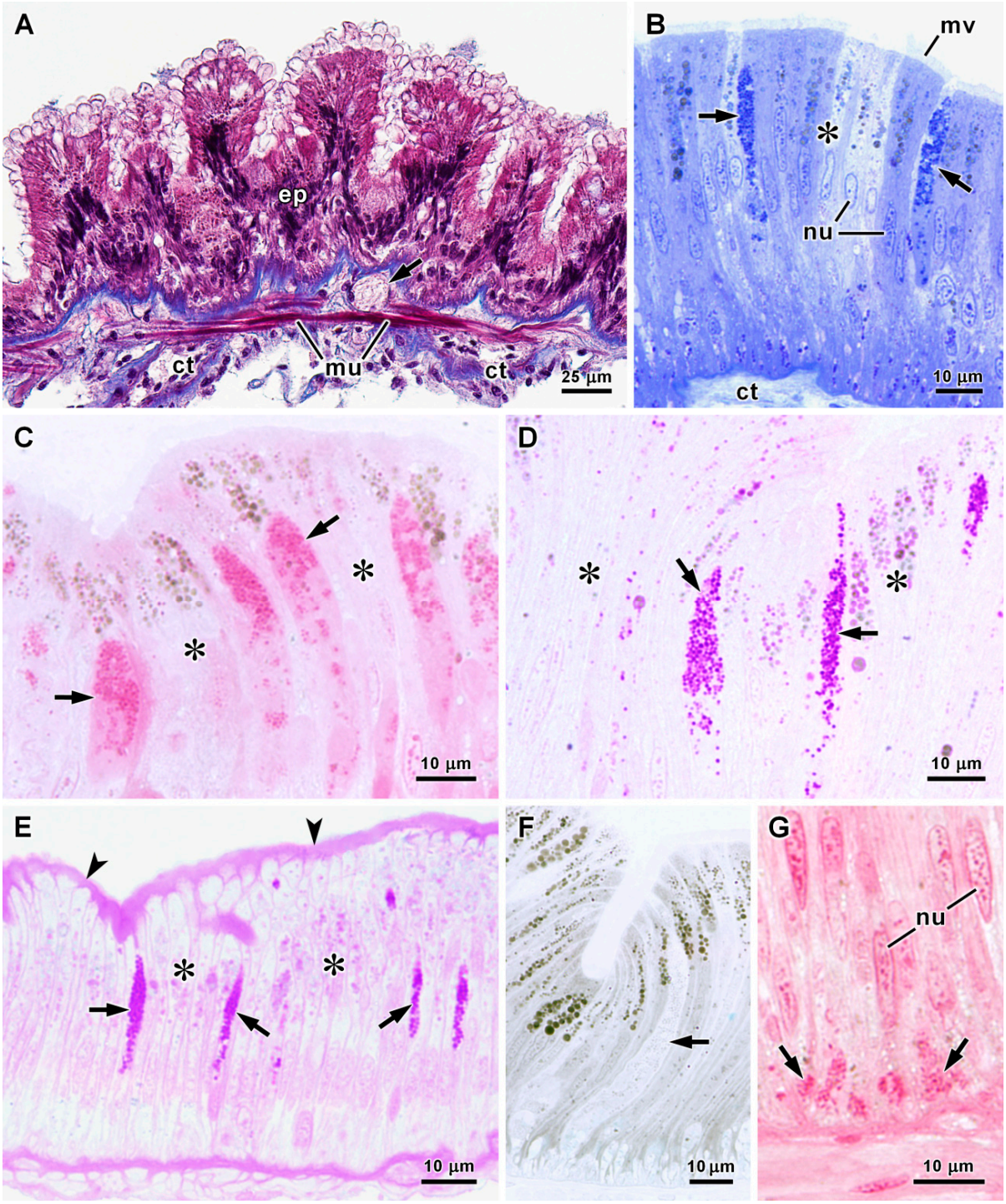

Figure 7. Stomach of *C. angulata* (**A**–**D**,**F**,**G**) and *A. fascicularis* (**E**) in histological (**A**) and semithin (**B**–**G**) sections. (**A**) Stomach wall stained by Masson's trichrome. A transverse section of a nerve (arrow) is visible below the epithelium (ep). (**B**–**D**) Absorptive cells (asterisks) and basophilic secretory cells (arrows) in the stomach of *C. angulata* stained by methylene blue and azure II (**B**), tetrazonium coupling reaction (**C**) and PAS reaction (**D**). (**E**) Secretory cells stained by PAS reaction (arrows) and absorptive cells (asterisks) in the stomach of *A. fascicularis*. The microvillous border is also stained (arrowheads). (**F**) Secretory cell (arrow) unstained by Alcian blue. (**G**) Basal cells (arrows) with vesicles stained by the tetrazonium coupling reaction. ct—connective tissue, mv—microvilli, mu—muscle fibres, nu—nuclei.

Transmission electron microscopy revealed the microvilli border of the stomach absorptive cells, but only some of them were ciliated. Vesicles, multivesicular bodies and many mitochondria were also observed in the apical region (Figure 8A). Lysosomes with variable sizes were abundant in the cytoplasm above the nucleus, and were stained with the electron-dense product of arylsulphatase detection (Figure 8B). Most lysosomes had diameters of 0.5–2.5 µm in ultrathin sections, but the largest ones that were found reached 5 µm. Some Golgi stacks and endoplasmic reticulum cisternae were also present. Glycogen deposits were abundant in most cells (Figure 8C), and especially in the basal region many peroxisomes were observed near mitochondria and lipid droplets. The peroxisomes of the stomach epithelium with 0.4–0.8 µm in diameter in ultrathin sections contained electron-dense inclusions in the matrix (Figure 8D). Deep cell membrane invaginations occurred in the basal region of the absorptive cells. The ultrastructural features of stomach secretory cells were identical in both species. Numerous electron-dense secretory vesicles occurred in the cytoplasm above the nucleus, with a tendency towards slightly larger vesicles in *A. fascicularis* (Table 1). Extensive Golgi stacks formed by cisternae with an electron-dense content and a great number of rough endoplasmic reticulum cisternae were other features of these cells (Figure 9A,B). Basal cells with oval electron-dense vesicles, identical to the basal cells of the oesophagus, were abundant in the stomach epithelium and in some ultrathin sections it was possible to observe close contact between nerves and basal cells (Figure 9C). A few intraepithelial neurons with a large round nucleus and many small electron-dense vesicles in the cytoplasm were also observed at the base of the stomach epithelium (Figure 9D).

3.4. Histology and Ultrastructure of the Intestine

Light microscopy observations of the intestine of both species revealed an epithelium with a wavy apical surface caused by differences in cell height. The intestinal epithelium ranged in height mostly between 40 µm and 100 µm and was largely formed by ciliated columnar absorptive cells (Figure 10A,B). The amount and intracellular distribution of lipid droplets in intestinal epithelial cells were variable, but numerous lipid droplets were frequently concentrated in the basal region of the absorptive cells (Figure 10C). Basophilic secretory cells containing small dark blue vesicles in semithin sections stained by methylene blue and azure II were present in the anterior intestine of both species (Figure 10D,E). Secretory cells in the anterior portion of *C. angulata* intestine were strongly stained by tetrazonium and PAS reactions (Figure 10F,G), but not by Alcian blue. On the other hand, in the anterior intestine of *A. fascicularis* secretory cells were stained by Alcian blue (Figure 10H) as well as by PAS and tetrazonium reactions (Table 1). In the valve between the anterior and posterior intestine of *A. fascicularis* the tall epithelial ridges further reduce the luminal space in this short narrow segment of the intestine (Figure 11A). Mucus-secreting cells with a basal nucleus were very abundant in the valve epithelium, alternating with very thin ciliated cells with a more apically located nucleus. This difference in the position of nuclei was more evident in thicker zones of the epithelium, in which two levels of nuclei were clearly visible (Figure 11A,B). In these mucous cells individualised secretory vesicles could not be recognized by light microscopy. Instead, a large mass of secretion moderately stained by methylene blue and azure II filled the cytoplasm. Most were strongly stained by PAS reaction (Figure 11C), but staining of histological sections with both PAS reaction and Alcian blue revealed heterogeneity among these mucous cells. Some were stained only by PAS reaction, others mainly by Alcian blue and still others showed double staining (Figure 11D). Secretion in these cells was weakly stained by the tetrazonium coupling reaction indicating a low protein content (Figure 11E). Secretory cells were rarely found in the posterior intestine of *A. fascicularis*, and were of the basophilic type as in the anterior intestine of this species. In *C. angulata* a very large number mucus-secreting cells strongly stained by Alcian blue were present in a short segment of the intestine that could correspond to the valve of *A. fascicularis* intestine. In the posterior intestine of *C. angulata* mucous cells were found in low numbers. These cells had a basal

nucleus and contained numerous vesicles unstained by methylene blue and azure II in semithin sections (Figure 11F). These secretory vesicles were strongly stained by Alcian blue (Figure 11G), but not at all by tetrazonium (Figure 11H) or PAS reactions (Table 1). Additionally, some basophilic cells were found in the posterior intestine of *C. angulata*. Basal cells were also observed in the intestinal epithelium of both species (Figure 10D). The outer layer of the intestine wall consisting of connective tissue, muscle cells and some nerves in general had a thickness of 15–25 µm, but only 5–15 µm in the posterior intestine of *A. fascicularis*.

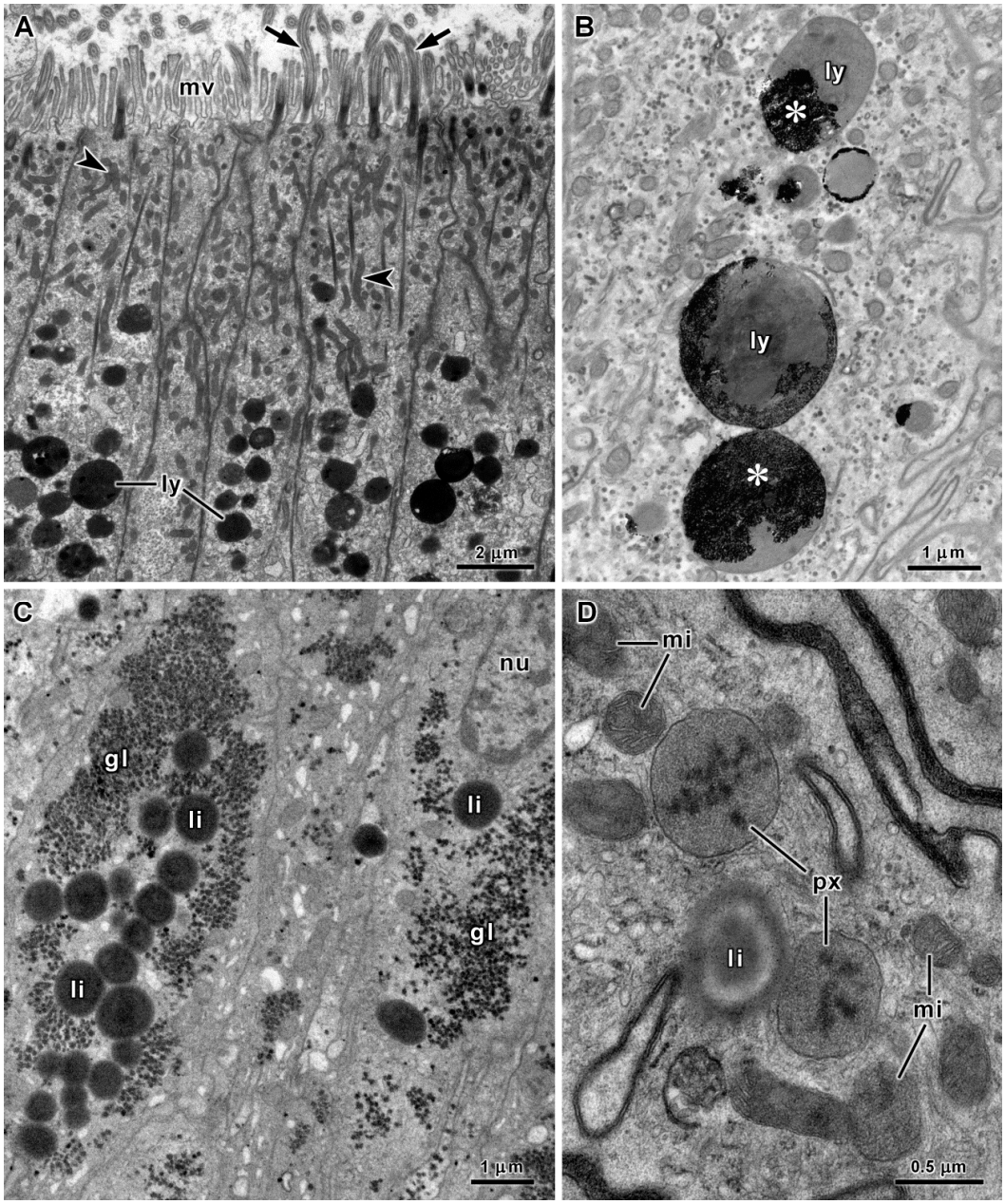

Figure 8. Ultrastructure of stomach absorptive cells in *C. angulata* (**A**,**B**) and *A. fascicularis* (**C**,**D**). (**A**) Apical region of the epithelium with a border of cilia (arrows) and microvilli (mv). Lysosomes (ly) and mitochondria (arrowheads) are abundant in the cytoplasm above the nucleus. (**B**) Lysosomes (ly) with electron-dense deposits (asterisks) resulting from arylsulphatase detection. (**C**) Glycogen deposits (gl) and lipid droplets (li) in the cytoplasm below the nucleus (nu). Ultrathin section stained with tannic acid and uranyl acetate. (**D**) Peroxisomes (px) in association with mitochondria (mi) and a lipid droplet (li).

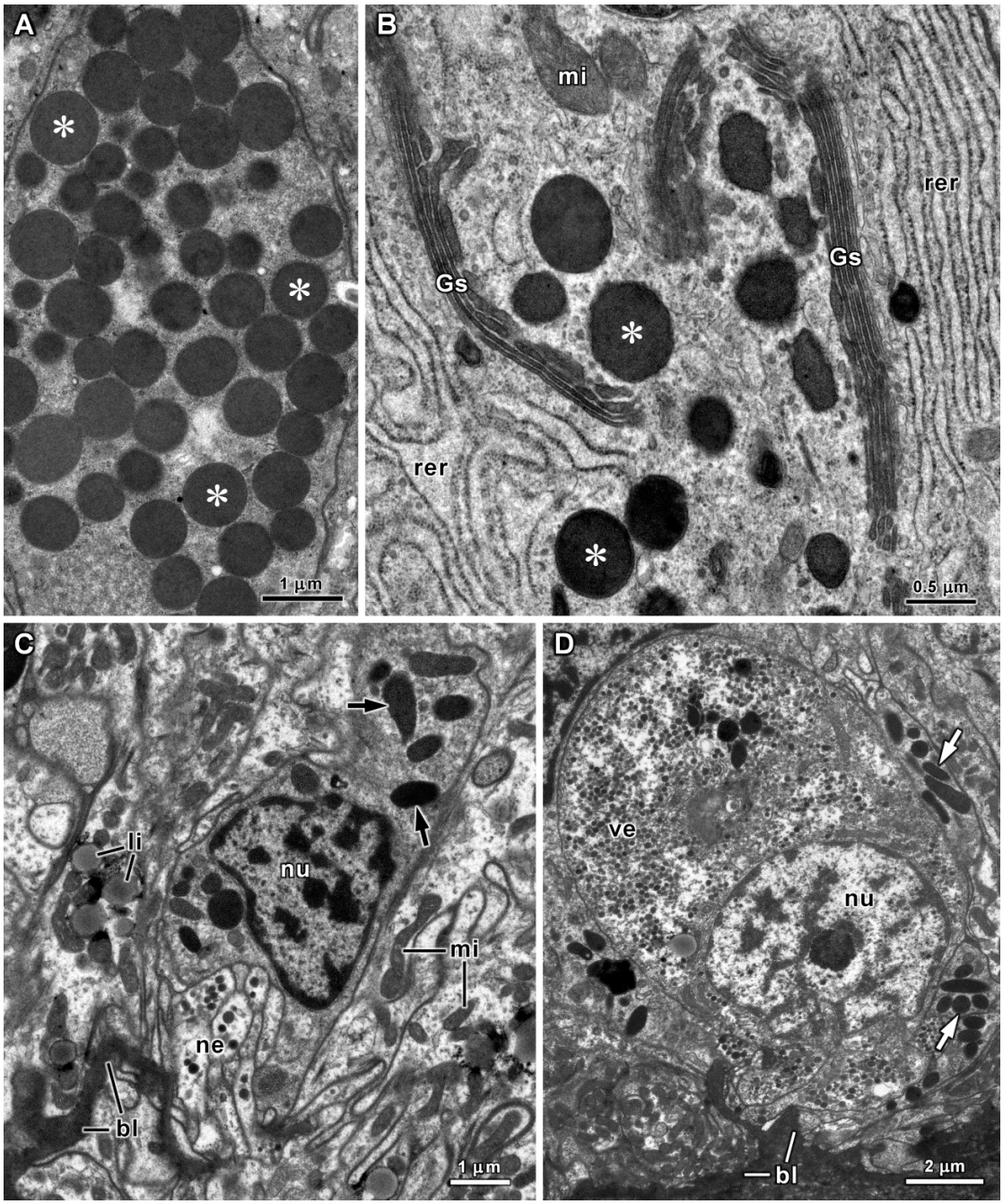

Figure 9. Ultrastructure of the stomach in *A. fascicularis* (**A**) and *C. angulata* (**B**–**D**). (**A**) Electron-dense vesicles (asterisks) in the apical region of a basophilic secretory cell. (**B**) Golgi stacks (Gs) and rough endoplasmic reticulum cisternae (rer) in a basophilic secretory cell containing electron-dense vesicles (asterisks). (**C**) Basal cell with electron-dense vesicles (arrows) in connection with a nerve terminal (ne). (**D**) Intraepithelial neuron with a large number of small vesicles (ve) in the cytoplasm. Basal cells with the electron-dense secretory vesicles (arrows) are visible around the neuron. bl—basal lamina, li—lipid droplets, mi—mitochondria, nu—nuclei.

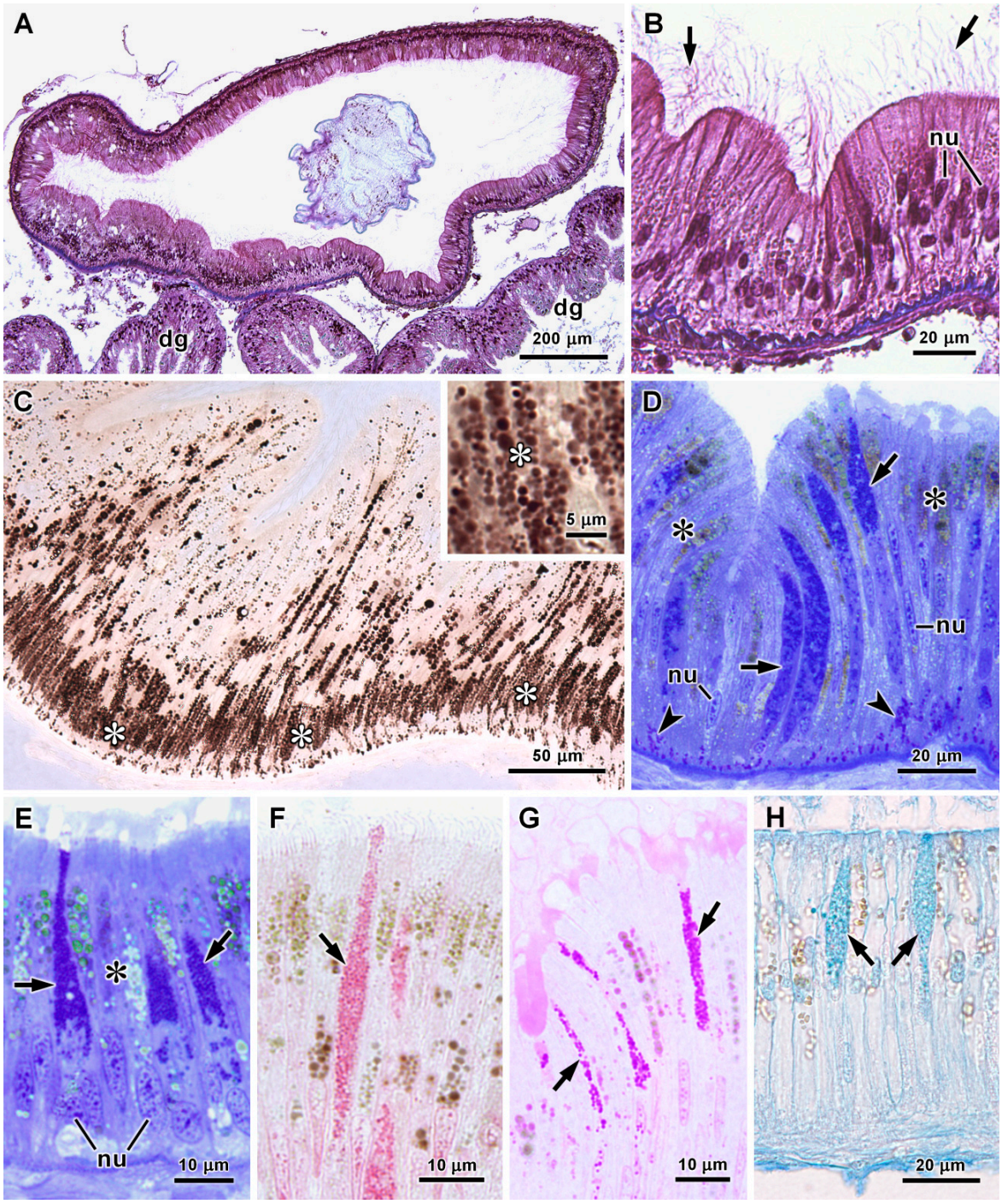

Figure 10. Intestine *C. angulata* (**A**–**D**,**F**,**G**) and *A. fascicularis* (**E**,**H**) in histological (**A**,**B**,**H**) and semithin (**C**–**G**) sections. (**A**,**B**) Transverse sections of the intestine stained by Masson's trichrome. The epithelium is covered by cilia (arrows in (**B**)). ((**C**), inset) Lipid droplets stained by Sudan black in the posterior intestine. Most lipid droplets (asterisks) are concentrated in the basal region of the absorptive cells. (**D**) Basophilic secretory cells (arrows), absorptive cells (asterisks) and basal cells (arrowheads) in the anterior intestine of *C. angulata*. Methylene blue and azure II staining. (**E**) Basophilic secretory cells (arrows) and absorptive cells (asterisk) in the anterior intestine of *A. fascicularis*. Methylene blue and azure II staining. (**F**,**G**) Secretory cells (arrows) stained by tetrazonium reaction (F) and PAS reaction (**G**) in the anterior intestine of *C. angulata*. (**H**) Secretory cells (arrows) stained by Alcian blue in the anterior intestine of *A. fascicularis*. dg—digestive gland, nu—nuclei.

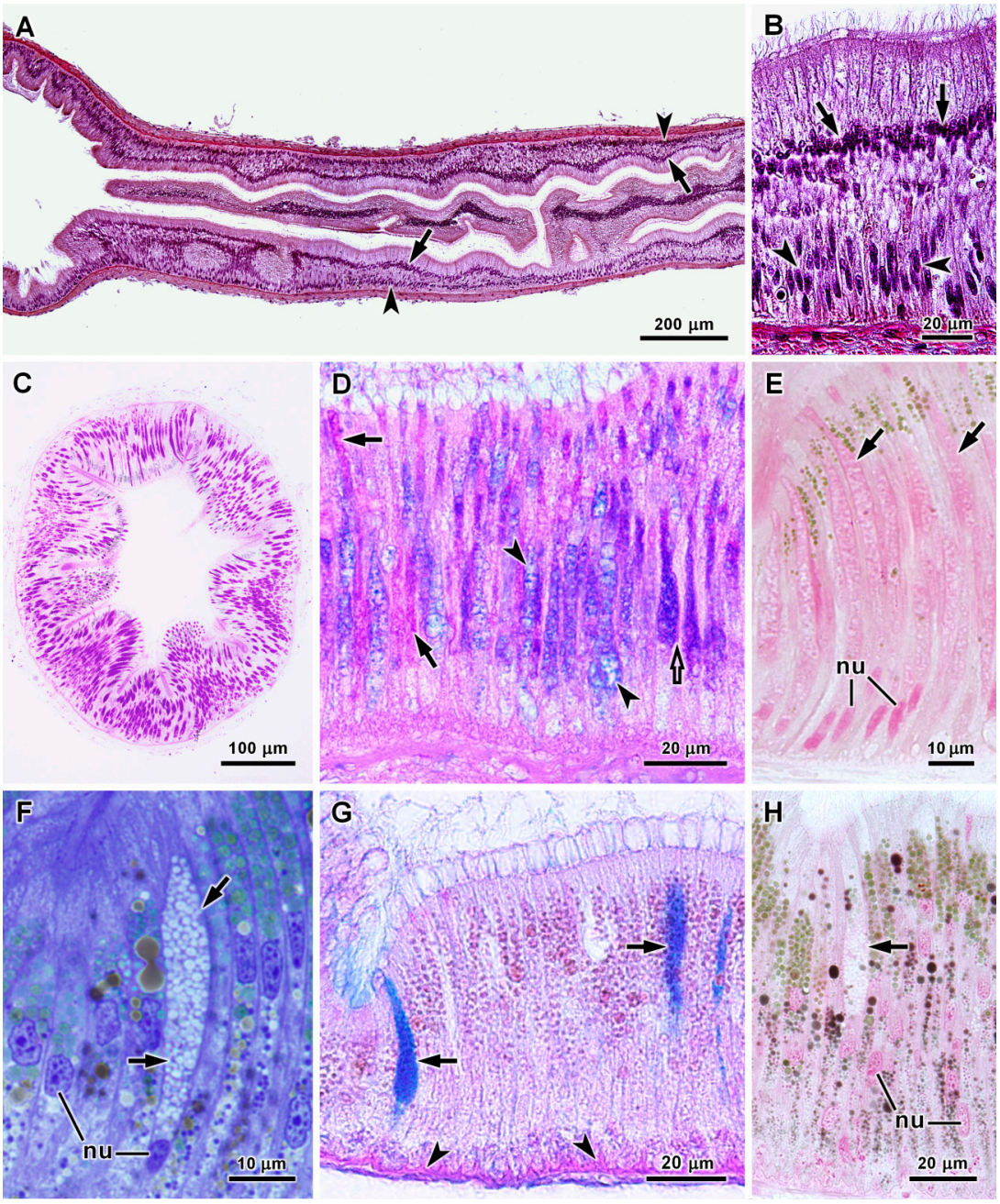

Figure 11. Intestine of *A. fascicularis* (**A**–**E**) and *C. angulata* (**F**–**H**) in histological (**A**,**B**,**D**,**G**) and semithin (**C**,**E**,**F**,**H**) sections. (**A**,**B**) Longitudinal (parasagittal) section of the valve between the anterior and posterior intestine of *A. fascicularis* stained by Masson's trichrome. The basal row of nuclei correspond to the nuclei of mucus-secreting cells (arrowheads) and the nuclei in the upper row belong to absorptive ciliated cells (arrows). (**C**) Transverse section of the valve with the mucus-secreting cells strongly stained by PAS reaction. (**D**) In the valve epithelium some mucus-secreting cell were stained only by PAS reaction (arrows), others mostly by Alcian blue (arrowheads) and still other were stained by both (open arrow). (**E**) Mucus-secreting cells of the valve (arrows) weakly stained by the tetrazonium coupling reaction. (**F**–**H**) Mucus-secreting cells (arrows) in the posterior intestine of *C. angulata*, unstained by methylene blue and azure II (**F**), strongly stained by Alcian blue (**G**) and unstained by the tetrazonium coupling reaction (**H**). The basal lamina is stained by PAS reaction (arrowheads in **G**). nu—nuclei.

As in other parts of the digestive tract, the absorptive cells of the intestine presented ultrastructural evidence of endocytic activity and intracellular digestion, namely, cell membrane pits, multivesicular bodies and lysosomes (Figure 12A–C). In *A. fascicularis* short cisternae with electron-dense content were present in the cytoplasm beneath the cell membrane, which were probably also related with endocytosis because a similar electron-dense content was found in multivesicular bodies (Figure 12A,B). In intestinal absorptive cells of both species mitochondria were abundant in the apical region in association with some peroxisomes. Lysosomes with electron-dense content were prominent in the cytoplasm above the nucleus and most had a diameter around 0.5–2.0 µm (Figure 12C), with the largest ones that were observed attaining about 3 µm in diameter. The detection of arylsulphatase activity in these organelles confirmed that they are active lysosomes. Deposits of glycogen granules were also present. Mainly in the posterior intestine, several peroxisomes were observed in association with large amounts of lipid droplets and mitochondria in the cytoplasm below the nucleus. These peroxisomes presented a granular matrix without cores (Figure 12D), and most had diameters of 0.5–1.5 µm in ultrathin sections.

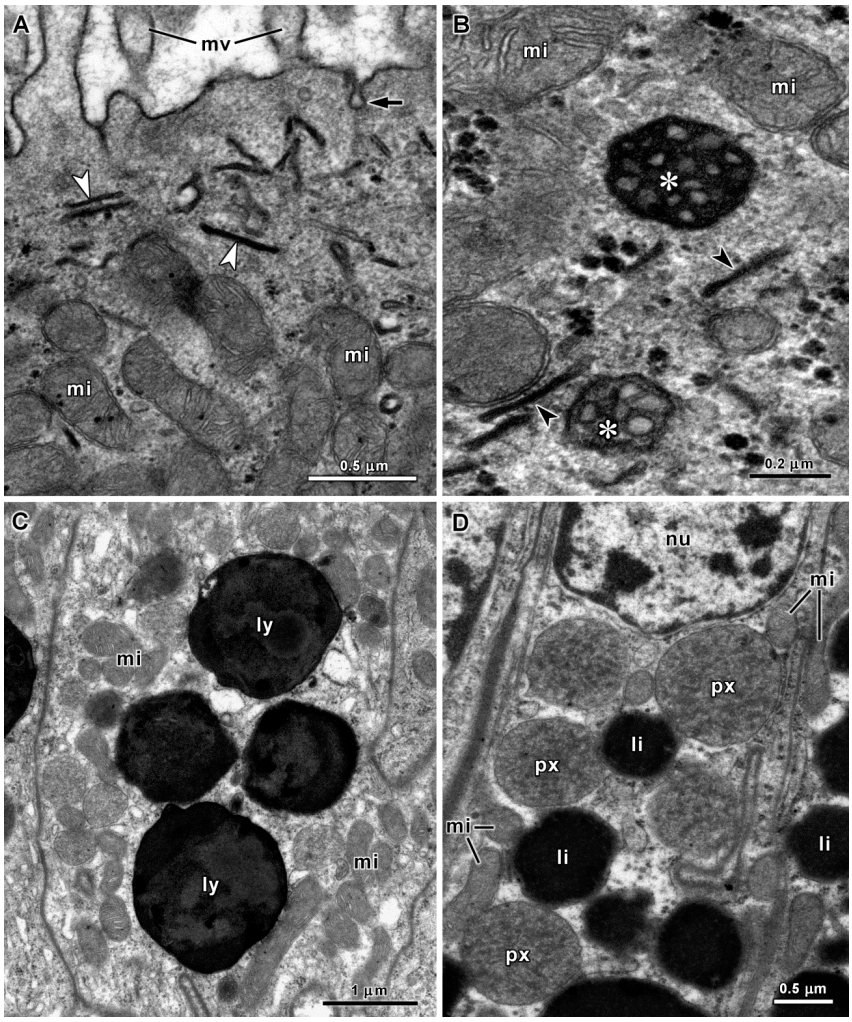

Figure 12. Ultrastructure of intestinal absorptive cells in *A. fascicularis* (**A**,**B**,**D**) and *C. angulata* (**C**). (**A**,**B**) A cell membrane pit (arrow), several mitochondria (mi), cisternae with electron-dense content (arrowheads) and multivesicular bodies (asterisks) in the apical region of absorptive cells. (**C**) Electron-dense lysosomes (ly) in the cytoplasm above de nucleus. (**D**) Several large peroxisomes (px) associated with lipid droplets (li) and mitochondria (mi) in the cytoplasm below the nucleus (nu). mi—mitochondria, mv—microvilli, nu—nucleus.

In both species, the secretory cells of the anterior intestine contained a large number of electron-dense vesicles (Figure 13A) with a tendency towards larger diameters in *A. fascicularis* (Table 1). These cells were rich in rough endoplasmic reticulum cisternae and the cisternae of their Golgi stacks had an electron-dense content (Figure 13B). In the valve between the anterior and posterior intestine of *A. fascicularis*, the mucus-secreting cells contained an accumulation of partially fused vesicles with flocculent material in an electron-lucent background, dilated rough endoplasmic reticulum cisternae and long Golgi stacks (Figure 13C,D). In the posterior intestine of *C. angulata* the cytoplasm of the mucus-secreting cells was almost entirely filled by round vesicles with low or median electron density. A few rough endoplasmic reticulum cisternae were present between the secretory vesicles (Figigue 14A). Some secretory cells with electron-dense secretory vesicles were also found in the posterior intestine of *A. fascicularis* (Figure 14B). However, in these secretory cells dome-shaped mitochondria (ring-shaped in some ultrathin sections) were frequently seen surrounding dilated rough endoplasmic reticulum cisternae (Figure 14C). This peculiar association between mitochondria and rough endoplasmic reticulum cisternae was not observed in any other cells of both species. Basal cells of the intestinal epithelium exhibited the same ultrastructural features and association with nerves observed in the oesophagus and stomach (Figure 14D).

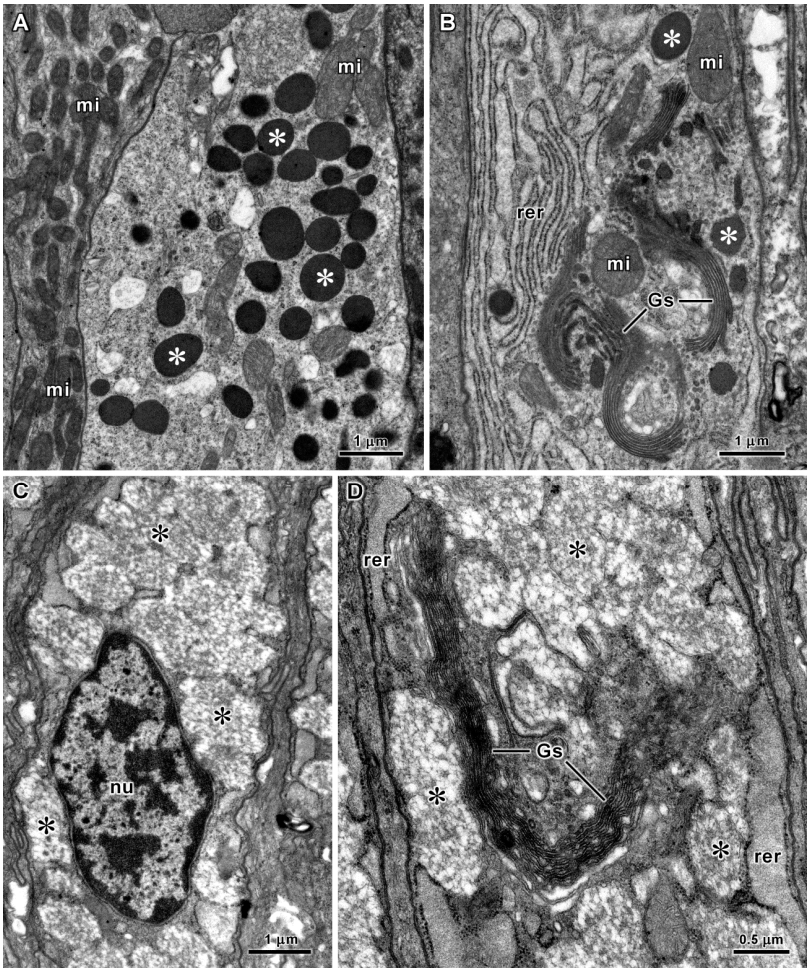

Figure 13. Ultrastructure of intestinal secretory cells in *C. angulata* (**A**,**B**) and *A. fascicularis* (**C**,**D**). (**A**,**B**) Electron-dense vesicles (asterisks), rough endoplasmic reticulum cisternae (rer) and Golgi stacks (Gs) in basophilic secretory cells of the anterior intestine. (**C**,**D**) Mucous cells of the valve between the anterior and posterior intestine in *A. fascicularis* with partially fused secretory vesicles (asterisks). These cells contain dilated rough endoplasmic reticulum cisternae (rer) and long Golgi stacks (Gs). nu—nucleus.

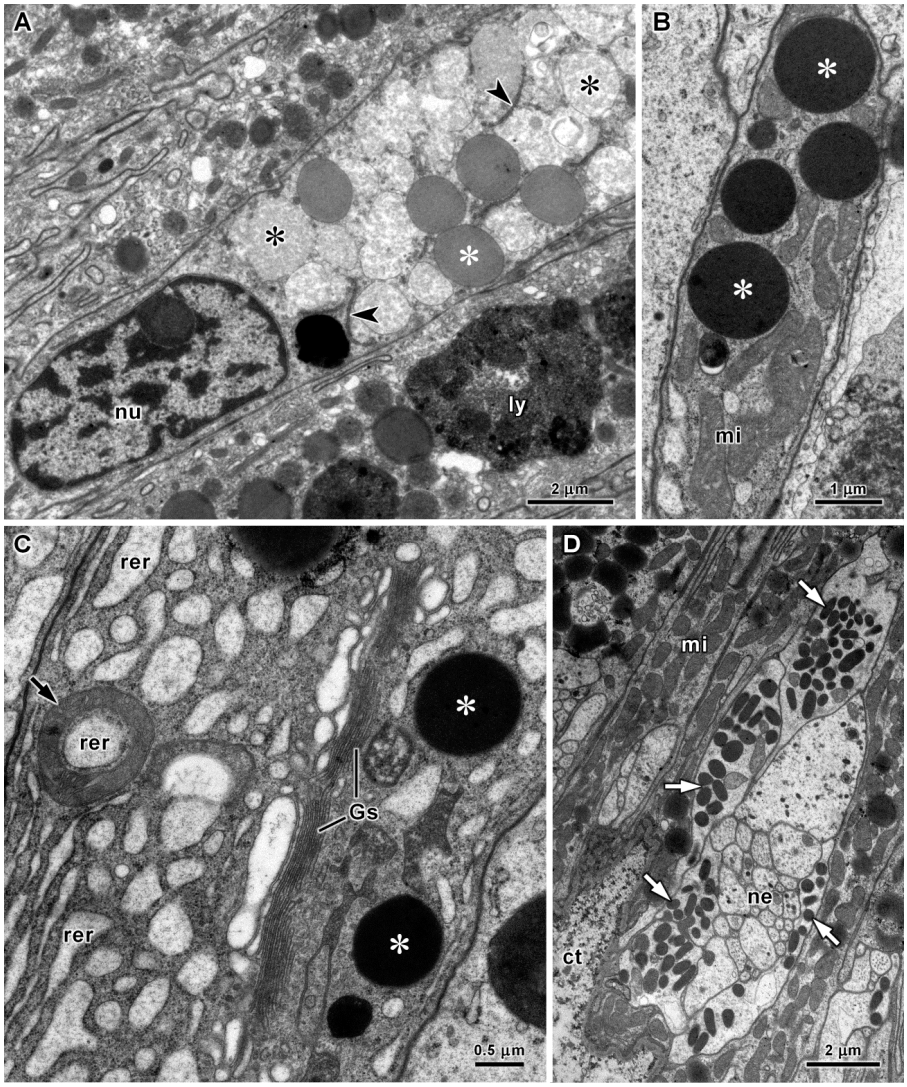

Figure 14. Ultrastructure of the posterior intestine in *C. angulata* (**A**) and *A. fascicularis* (**B**–**D**). (**A**) Mucus-secreting cell with vesicles of low and median electron density (asterisks) and a few rough endoplasmic reticulum cisternae (arrowheads). (**B**) Apical region of a narrow basophilic cell with electron-dense secretory vesicles (asterisks). (**C**) Electron-dense vesicles (asterisks), rough endoplasmic reticulum cisternae (rer), Golgi stacks (Gs) and a mitochondrion with a ring-shaped section (arrow) surrounding a portion of endoplasmic reticulum in a basophilic secretory cell. (**D**) Basal cells with oval electron-dense vesicles (arrows) around an intraepithelial nerve terminal (ne). ct—connective tissue, ly—lysosome, mi—mitochondria, nu—nucleus.

4. Discussion

This article presents the results of the first histochemical and ultrastructural investigation of the oesophagus, stomach and intestine of chitons. The species *Chaetopleura angulata* and *Acanthochitona fascicularis* were chosen for this propose because they were previously employed for the study of the oesophageal pouches [9]. Both species occur intertidally on the Portuguese coast and are common at the collection site. They belong, respectively, to the families Chaetopleuridae (suborder Chitonina) and Acanthochitonidae (suborder Acanthochitonina) of the order Chitonida that comprises around 80% of the living species of chitons [23]. The stomach content of the two species revealed a diversified omnivorous diet, supporting the growing evidence that in general intertidal chitons are omnivorous [11,12]. Previous reports indicated the consumption of barnacles by *C. angulata* and based on that information the species was classified as carnivorous [24], but the present

results clearly show that it is omnivorous. The ingestion of small crustaceans by *C. angulata* was confirmed, but remains of invertebrates were not found in the digestive tract of *A. fascicularis*. Although substantial amounts of unidentifiable residues were present, algae largely predominated in the stomach content of the *A. fascicularis* specimens that were analysed. Additionally, the intestine-body length ratios of the species included in this study (2.4–3.0) fit well within the ratios found for other omnivorous chitons [8].

The digestive process is still much less studied in polyplacophorans than in gastropods, bivalves or cephalopods [25]. Nevertheless, it is recognized that digestion in polyplacophorans follows the general pattern known for other molluscs, starting in the lumen of the digestive tract with secreted enzymes and ending intracellularly in lysosomes. As in other chitons [5] and generally in molluscs [26], the digestive tract epithelium in *C. angulata* and *A. fascicularis* consists of ciliated and non-ciliated columnar absorptive cells and secretory cells. The observation of cell membrane pits, vesicles and multivesicular bodies, which belong to the endolysosomal system [27], are indicative of endocytosis in the apical region of absorptive cells as experimentally demonstrated in other molluscs [28–30]. By this process, ultrafine nutritive particles resulting from extracellular digestion in the digestive tract lumen are introduce in the absorptive cells to be digested in lysosomes [31], which are abundant organelles in the entire digestive tract epithelium of these two species of chitons, as well as in their oesophageal pouches [9]. Additionally, small molecules such as simple sugars and amino acids can be absorbed directly through the cell membrane of the microvilli border of the digestive tract epithelium, as demonstrated in other molluscs [28,29,32]. Although in molluscs the digestive gland is considered the main site of nutrient absorption, intracellular digestion and storage of reserves, these functions are shared with epithelial cells of the digestive tract [26]. Mitochondria were particularly abundant in the apical and basal regions of absorptive cells. In the apical region, these organelles must be required to supply energy for ciliary motion and endocytosis. The concentration of mitochondria in the basal region of the digestive tract epithelium also denotes a need for high ATP production in this region, naturally required for active transport of metabolites and ions across the basal cell membrane. Moreover, the required energy can be obtained from glycogen and lipid reserves that are present in absorptive cells. The association of lipid droplets with peroxisomes mainly at the basal region of absorptive cells suggests the use of fatty acids to produce acetyl-CoA through peroxisomal β-oxidation, in order to fuel the citric acid cycle in nearby mitochondria and ultimately produce ATP [33]. Data are not available for polyplacophorans, but fatty acid β-oxidation is a standard metabolic pathway of peroxisomes [34]. Enzymes of this pathway were detected in mussel peroxisomes [35,36] and should also be present in digestive system of other molluscs. Although not always present, electron-dense crystalline cores are common in peroxisomes of molluscs and other taxa [37–39], and were found in peroxisomes of absorptive cells in *A. fascicularis* oesophageal pouches [9] and in peroxisomes of chiton digestive gland [7]. However, cores were not seen in digestive tract peroxisomes of *A. fascicularis* and *C. angulata*, in which only some electron-dense spots were observed in the peroxisomal matrix. In molluscs, peroxisomes are usually larger and more abundant in the digestive gland [7,37–39]. Peroxisomes not exciding 0.5 µm in diameter closely associated with mitochondria and lipid droplets were reported in digestive tract epithelial cell of gastropods [40–43]. However, in the intestine of *A. fascicularis* and *C. angulata* peroxisomes are larger and numerous, denoting a higher importance of peroxisomal metabolism in these cells where lipid reserves are often abundant.

Though the absorptive cells of the digestive tract epithelium were found to be similar in these two species of chitons, some differences were detected in their secretory cells. Secretory cells in the digestive tract of *A. fascicularis* and *C. angulata* can be divided in two main categories: basophilic and mucous. Cells containing secretory vesicles with high electron density when observed by transmission electron microscopy and displaying a dark blue colour in semithin sections stained by methylene blue and azure II were designated as basophilic cells. This designation is applied to the secretory cells of the digestive

gland responsible for secretion of enzymes for extracellular digestion in molluscs [26], and was also used for one type of secretory cells of the glandular oesophageal pouches of chitons that could as well be responsible for secretion of digestive enzymes [9]. These cells containing electron-dense secretory vesicles with a high protein concentration are rich in rough endoplasmic reticulum cisternae and could be considered serous cells [44]. However, the histochemical methods indicate that the secretory vesicles of chiton basophilic cells are also rich in polysaccharides, and in some cases including acidic polysaccharides that are more typical of mucus-secreting cells. Secretory cells with serous features were also found in the digestive tract of other molluscs, and although precise knowledge about their functions are still lacking they could be responsible for secretion of some digestive enzymes [45–48]. In alternative, it was also suggested that intestinal secretory cells could produce a proteinaceous cement to coat the faecal rods with a protective layer to prevent their disintegration [32]. Mucous cells typically contain secretory vesicles with low electron-density rich in acid polysaccharides [49]. Mucous cells are abundant in the digestive tract of several herbivorous gastropods [43,45,48,50,51] and in the oesophageal pouches of *A. fascicularis* and *C. angulata* [9]. However, cells of this type were not common in the digestive tract of these two chiton species, except in the intestinal valve where mucous cells were very abundant. Mucous secretion can protect the digestive tract epithelium and agglutinate particles. It is also known that mucin MUC2 secreted by vertebrate intestinal goblet cells is a highly glycosylated glycoprotein with immunoregulatory functions [52]. Thus, secretion of glycoproteins with defensive and regulatory activities is another possible function for the intestinal secretory cells of chitons and other molluscs. Therefore, without further knowledge about the precise physiological role of the different secretory cell types found in the digestive tract of chitons and other molluscs it is not possible to evaluate the full meaning of the histological differences concerning these cells.

The basal cells that were observed throughout the digestive tract epithelium of *C. angulata* and *A. fascicularis* presented histological and ultrastructural features of enteroendocrine cells, namely, clear cytoplasm and basally located electron-dense secretory vesicles (also called secretory granules) [53,54]. Morphologically identical basal cells were recently reported in the oesophageal pouches of these two chitons species [9]. However, these cells that are detectable in semithin sections were not mentioned in earlier histological studies of polyplacophoran digestive system [5], probably because they are not evident in classical histological sections. Enteroendocrine cells occur along the digestive tract of both vertebrates and invertebrates, and produce peptidic hormones that are accumulated in secretory vesicles ready to be released at the base of the epithelium in response to specific stimuli [55,56]. Hence, the histochemical detection of proteic substances in the vesicles of chiton basal cells by the tetrazonium coupling reaction is compatible with the production and storage of peptidic hormones in these cells. The presence of endocrine cells in the digestive tract epithelium of gastropods and bivalves was confirmed by immunostaining with antibodies against vertebrate peptidic hormones such as insulin, gastrin, somatostatin and glucagon [46,57–59]. More recently, insulin related peptides were identified and sequenced in some molluscs and other invertebrates [60]. Therefore, similar hormones should also be produced by the enteroendocrine cells of polyplacophorans for metabolic regulation. In the digestive tract of gastropods and bivalves enteroendocrine cells are isolated and scattered in the epithelium [43,46,57,59,61]. In mammals these cells are also rare and dispersed, corresponding to less than 1% of the total epithelial cells of the intestine [56,62]. Conversely, the enteroendocrine-like basal cells are numerous in the entire digestive tract of chitons, forming a distinct layer at the base of the epithelium. Since contact of these cells with the digestive tract lumen was not observed, at least most of them must be enteroendocrine cells of the closed type. Enteroendocrine cells of the open type reach the digestive tract lumen and can release hormones in direct response to the molecules present in the lumen, whereas enteroendocrine cells of close type are believed to be indirectly activated by those chemical stimuli [55]. In the intestine of the freshwater snail *Planorbarius corneus* and the sea hare *Aplysia depilans* the enteroendocrine cells also appear to be isolated from the lumen [43,46].

However, in the land snail *Helix aspersa* and in freshwater bivalves the apical process of the enteroendocrine cells reached the lumen of the intestine [57,61]. In the intestine of the gastropod *Vivaparus ater* both close and open types of enteroendocrine cells were reported [59]. Another important aspect is the connection between the enteroendocrine cells and nerves, which was frequently observed along the digestive tract of *C. angulata* and *A. fascicularis*, as in other molluscs [43,46,61]. Due to these connections, enteroendocrine cells are a fundamental component of a neuroepithelial circuit that provides an interaction between the digestive tract and the nervous system [63].

The main histological differences between the digestive tract of *C. angulata* and *A. fascicularis* concern the secretory cells. These histological differences could be related to diet or being due to the taxonomic distance between these species that belong to different suborders. Although both species included in this study consume foraminiferans, unicellular and multicellular algae, remains of crustaceans were found only in the stomach of *C. angulata*. However, without data on other chiton species with similar and distinct diets it is premature to establish a correlation between feeding habits and digestive system histology.

Supplementary Materials: The following supporting information was downloaded at: https://www.mdpi.com/article/10.3390/jmse10020160/s1, Figure S1: Species and collection site. (A,B) Location of the collection site (arrows). (C,D) Specimens of *Chaetopleura angulata* (C) and *Acanthochitona fascicularis* (D) on roof tiles that were dumped in large amounts at the collection site and are now colonized by intertidal species.

Author Contributions: A.L.-d.-C. research and writing; G.C., Â.A. and E.O. research. All authors have read and agreed to the published version of the manuscript.

Funding: The study was supported by funding from the Institute of Biomedical Sciences Abel Salazar (ICBAS) of the University of Porto (Portugal), and FCT—Fundação para a Ciência e a Tecnologia (Portugal), through the strategic project UIDB/04292/2020 granted to MARE.

Institutional Review Board Statement: Not required in this case.

Informed Consent Statement: Not applicable.

Data Availability Statement: Microscopy slides kept in the Department of Microscopy (ICBAS-UP, Porto, Portugal) can be consulted on request.

Acknowledgments: The authors thank Paula Teixeira and Aurora Rodrigues for technical assistance.

Conflicts of Interest: The authors declare no conflict of interest.

References

1. Eernisse, D.J.; Reynolds, P.D. Polyplacophora. In *Microscopic Anatomy of Invertebrates*; Harrison, F.W., Kohn, A.J., Mollusca, I., Eds.; Wiley-Liss: New York, NY, USA, 1994; Volume 5, pp. 55–110.
2. Todt, C.; Okusu, A.; Schander, C.; Schwabe, E. Solenogastres, Caudofoveata, and Polyplacophora. In *Phylogeny and Evolution of the Mollusca*; Ponder, W.F., Lindberg, D.R., Eds.; University of California Press: Berkeley, CA, USA, 2008; pp. 71–96.
3. Sigwart, J.D.; Vermeij, G.J.; Hoyer, P. Why do chitons curl into a ball? *Biol. Lett.* **2019**, *15*, 20190429. [CrossRef] [PubMed]
4. Ponder, W.F.; Lindberg, D.R.; Ponder, J.M. *Biology and Evolution of the Mollusca*; CRC Press: Boca Raton, FL, USA, 2020; Volume 2.
5. Fretter, V. The structure and function of the alimentary canal of some species of Polyplacophora (Mollusca). *Trans. R. Soc. Edin.* **1937**, *49*, 119–164. [CrossRef]
6. Greenfield, M.L. Feeding and gut physiology in *Acanthopleura spinigera* (Mollusca). *J. Zool. Lond.* **1972**, *166*, 37–47. [CrossRef]
7. Lobo-da-Cunha, A. The peroxisomes of the hepatopancreas in two species of chitons. *Cell Tissue Res.* **1997**, *290*, 655–664. [CrossRef]
8. Sigwart, J.D.; Schwabe, E. Anatomy of the many feeding types in polyplacophoran molluscs. *Invert. Zool.* **2017**, *14*, 205–216. [CrossRef]
9. Lobo-da-Cunha, A.; Alves, A.; Oliveira, E.; Calado, G. Functional morphology of the glandular esophageal pouches of chitons (Mollusca, Polyplacophora). *J. Morphol.* **2021**, *282*, 355–367. [CrossRef]
10. Latyshev, N.A.; Khardin, A.S.; Kasyanov, S.P.; Ivanova, M.B. A study on the feeding ecology of chitons using analysis of gut contents and fatty acid markers. *J. Moll. Stud.* **2004**, *70*, 225–230. [CrossRef]
11. Camus, P.; Daroch, K.; Opazo, L. Potential for omnivory and apparent intraguild predation in rocky intertidal herbivore assemblages from northern Chile. *Mar. Ecol. Progr. Ser.* **2008**, *361*, 35–45. [CrossRef]

12. Camus, P.; Arancibia, P.; Ávila-Thieme, M. A trophic characterization of intertidal consumers on Chilean rocky shores. *Rev. Biol. Mar. Oceanogr.* **2013**, *48*, 431–450. [CrossRef]
13. Saito, H.; Okutani, T. Carnivorous habits of two species of the genus *Craspedochiton* (Polyplacophora: Acanthochitonidae). *J. Malacol. Soc. Aust.* **1992**, *13*, 55–63. [CrossRef]
14. Duperron, S.; Pottier, M.-A.; Léger, N.; Gaudron, S.M.; Puillandre, N.; Le Prieur, S.; Sigwart, J.D.; Ravaux, J.; Zbinden, M. A tale of two chitons: Is habitat specialisation linked to distinct associated bacterial communities? *FEMS Microbiol. Ecol.* **2013**, *83*, 552–567. [CrossRef] [PubMed]
15. Brooker, L.R.; Shaw, J. The chiton radula: A unique model for biomineralization studies. In *Advanced Topics in Biomineralization*; Seto, J., Ed.; InTech: Rijeka, Croatia, 2012; pp. 65–84. [CrossRef]
16. Boyle, P.R. Fine structure of the subradular organ of Lepidochitona cinereus (L), (Mollusca, Polyplacophora). *Cell Tissue Res.* **1975**, *162*, 411–417. [CrossRef] [PubMed]
17. Meeuse, B.J.D.; Fluegel, W. Carbohydrate-digesting enzymes in the sugar gland juice of Cryptochiton stelleri. *Arch. Neerl. Zool.* **1958**, *13*, 301–313. [CrossRef]
18. Saito, H.; Okutani, T. Taxonomy of Japanese species of the genera *Mopalia* and *Plaxiphora* (Polyplacophora: Mopaliidae). *Veliger* **1991**, *34*, 172–194.
19. Sannes, P.L.; Katsuyama, T.; Spicer, S. Tannic acid-metal salt sequences for light and electron microscopic localization of complex carbohydrates. *J. Histochem. Cytochem.* **1978**, *26*, 55–61. [CrossRef]
20. Ganter, P.; Jollès, G. *Histochimie Normal et Pathologique*; Gauthier-Villars: Paris, France, 1970.
21. Lane, B.P.; Europa, D.L. Differential staining of ultrathin sections of Epon-embedded tissues for light microscopy. *J. Histochem. Cytochem.* **1965**, *13*, 579–582. [CrossRef]
22. Hopsu-Havu, V.K.; Arstila, A.V.; Helminen, H.J.; Kalimo, H.O. Improvements in method for electron microscopic localization of arylsulphatase activity. *Histochemie* **1967**, *8*, 54–64. [CrossRef]
23. Sigwart, J.D.; Stoeger, I.; Knebelsberger, T.; Schwabe, E. Chiton phylogeny (Mollusca: Polyplacophora) and the placement of the enigmatic species *Choriplax grayi* (H. Adams & Angas). *Invertebr. Syst.* **2013**, *27*, 603–621. [CrossRef]
24. Kaas, P.; Van Belle, R.A. Monograph of living chitons (Mollusca: Polyplacophora). In *Suborder Ischnochitonina, Ischnochitonidae: Chaetopleurinae & Ischnochitoninae (pars)*; E. J. Brill and W. Backhuys: Leiden, The Netherlands, 1987; Volume 3.
25. Ponder, W.F.; Lindberg, D.R.; Ponder, J.M. *Biology and Evolution of the Mollusca*; CRC Press: Boca Raton, FL, USA, 2020; Volume 1.
26. Lobo-da-Cunha, A. Structure and function of the digestive system in molluscs. *Cell Tissue Res.* **2019**, *377*, 475–503. [CrossRef]
27. Klumperman, J.; Raposo, G. The complex ultrastructure of the endolysosomal system. *Cold Spring Harb. Perspect. Biol.* **2014**, *6*, a016857. [CrossRef]
28. Walker, G. The digestive system of the slug, *Agriolimax reticulatus* (Müller): Experiments on phagocytosis and nutrient absorption. *Proc. Malacol. Soc. Lond.* **1972**, *40*, 33–43. [CrossRef]
29. Bush, M.S. The ultrastructure and function of the oesophagus of *Patella vulgata*. *J. Moll. Stud.* **1989**, *55*, 111–124. [CrossRef]
30. Bourne, N.B.; Jones, W.; Bowen, I.D. Endocytosis in the crop of the slug, Deroceras reticulatum (Müller) and the effects of the ingested molluscicides, metaldehyde and methiocarb. *J. Moll. Stud.* **1991**, *57*, 71–80. [CrossRef]
31. Huotari, J.; Helenius, A. Endosome maturation. *EMBO J.* **2011**, *30*, 3481–3500. [CrossRef] [PubMed]
32. Bush, M.S. The ultrastructure and function of the intestine of *Patella vulgata*. *J. Zool.* **1988**, *215*, 685–702. [CrossRef]
33. Schrader, M.; Kamoshita, M.; Islinger, M. Organelle interplay - peroxisome interactions in health and disease. *J. Inherit. Metab. Dis.* **2020**, *43*, 71–89. [CrossRef] [PubMed]
34. Islinger, M.; Cardoso, M.J.R.; Schrader, M. Be different—The diversity of peroxisomes in the animal kingdom. *Biochim. Biophys. Acta Mol. Cell Res.* **2010**, *1803*, 881–897. [CrossRef]
35. Cajaraville, M.P.; Völkl, A.; Fahimi, H.D. Peroxisomes in the digestive gland cells of the mussel *Mytilus galloprovincialis* Lmk. Biochemical, ultrastructural and immunocytochemical characterization. *Europ. J. Cell Biol.* **1992**, *56*, 255–264.
36. Cancio, I.; Völkl, A.; Beier, K.; Fahimi, H.D.; Cajaraville, M.P. Peroxisomes in molluscs, characterization by subcellular fractionation combined with western blotting, immunohistochemistry, and immunocytochemistry. *Histochem. Cell Biol.* **2000**, *113*, 51–60. [CrossRef]
37. Owen, G. Lysosomes, peroxisomes and bivalves. *Sci. Prog.* **1972**, *60*, 299–318.
38. Lobo-da-Cunha, A.; Batista, C.; Oliveira, E. The peroxisomes of the hepatopancreas in marine gastropods. *Biol. Cell* **1994**, *82*, 67–74. [CrossRef]
39. Lobo-da-Cunha, A.; Oliveira, E.; Alves, A.; Calado, G. Giant peroxisomes revealed by a comparative microscopy study of digestive gland cells of cephalaspidean sea slugs (Gastropoda, Euopisthobranchia). *J. Mar. Biol. Assoc.* **2019**, *99*, 197–202. [CrossRef]
40. Triebskorn, R. Ultrastructural changes in the digestive tract of *Deroceras reticulatum* (Müller) induced by a carbamate molluscicide and by metaldehyde. *Malacologia* **1989**, *31*, 141–156.
41. Lobo-da-Cunha, A.; Batista-Pinto, C. Stomach cells of *Aplysia depilans* (Mollusca, Opisthobranchia): A histochemical, ultrastructural, and cytochemical study. *J. Morphol.* **2003**, *256*, 360–370. [CrossRef] [PubMed]
42. Lobo-da-Cunha, A.; Batista-Pinto, C. Light and electron microscopy studies of the oesophagus and crop epithelium in *Aplysia depilans* (Mollusca, Opisthobranchia). *Tissue Cell* **2005**, *37*, 447–456. [CrossRef] [PubMed]
43. Lobo-da-Cunha, A.; Batista-Pinto, C. Ultrastructural, histochemical and cytochemical characterisation of intestinal epithelial cells in *Aplysia depilans* (Gastropoda, Opisthobranchia). *Acta Zool.* **2007**, *88*, 211–221. [CrossRef]

44. Tandler, B.; Phillips, C.J. Structure of serous cells in salivary glands. *Microsc. Res. Tech.* **1993**, *26*, 32–48. [CrossRef]
45. Boer, H.H.; Kits, K.S. Histochemical and ultrastructural study of the alimentary tract of the freshwater snail *Lymnaea stagnalis*. *J. Morphol.* **1990**, *205*, 97–111. [CrossRef]
46. Franchini, A.; Ottaviani, E. Intestinal cell types in the freshwater snail *Planorbarius corneus*: Histochemical, immunocytochemical and ultrastructural observations. *Tissue Cell.* **1992**, *24*, 387–396. [CrossRef]
47. Pfeiffer, C.J. Intestinal ultrastructure of *Nerita picea* (Mollusca: Gastropoda), an Intertidal marine snail of Hawaii. *Acta Zool.* **1992**, *73*, 39–47. [CrossRef]
48. Lobo-da-Cunha, A.; Malheiro, A.R.; Alves, A.; Oliveira, E.; Coelho, R.; Calado, G. Histological and ultrastructural characterisation of the stomach and intestine of the opisthobranch *Bulla striata* (Heterobranchia: Cephalaspidea). *Thalassas* **2011**, *27*, 61–75.
49. Tandler, B. Structure of mucous cells in salivary glands. *Microsc. Res. Tech.* **1993**, *26*, 49–56. [CrossRef] [PubMed]
50. Lobo-da-Cunha, A.; Oliveira, E.; Ferreira, I.; Coelho, R.; Calado, G. Histochemical and ultrastructural characterization of the posterior esophagus of *Bulla striata* (Mollusca, Opisthobranchia). *Microsc. Microanal.* **2010**, *16*, 688–698. [CrossRef] [PubMed]
51. Leal-Zanchet, A.M. Ultrastructure of the supporting cells and secretory cells of the alimentary canal of the slugs, *Lehmannia marginata* and *Boettgerilla pallens* (Pulmonata: Stylommatophora: Limacoidea). *Malacologia* **2002**, *44*, 223–239.
52. Shan, M.M.; Gentile, M.; Yeiser, J.R.; Walland, A.C.; Bornstein, V.U.; Chen, K.; He, B.; Cassis, L.; Bigas, A.; Cols, M.; et al. Mucus enhances gut homeostasis and oral tolerance by delivering immunoregulatory signals. *Science* **2013**, *342*, 447–453. [CrossRef]
53. Portela-Gomes, G.M.; Grimelius, L.; Bergström, R. Enterochromaffin (argentaffin) cells of the rat gastrointestinal tract. An ultrastructural study. *Acta Pathol. Microbiol. Immunol. Scand. A* **1984**, *92*, 83–89. [CrossRef]
54. Wade, P.R.; Westfall, J.A. Ultrastructure of enterochromaffin cells and associated neural and vascular elements in the mouse duodenum. *Cell Tissue Res.* **1985**, *241*, 557–563. [CrossRef]
55. Latorre, R.; Sternini, C.; De Giorgio, R.; Greenwood-Van Meerveld, B. Enteroendocrine cells: A review of their role in brain-gut communication. *Neurogastroenterol. Motil.* **2016**, *28*, 620–630. [CrossRef]
56. Guo, X.; Lv, J.; Xi, R. The specification and function of enteroendocrine cells in *Drosophila* and mammals: A comparative review. *FEBS J.* **2021**, *epublication ahead of print*. [CrossRef]
57. Plisetskaya, E.; Kazakov, V.K.; Soltitskaya, L.; Leibson, L.G. Insulin-producing cells in the gut of freshwater bivalve mollusks *Anodonta cygnea* and *Unio pictorum* and the role of insulin in the regulation of their carbohydrate metabolism. *Gen. Comp. Endocrinol.* **1978**, *35*, 133–145. [CrossRef]
58. Marchand, C.R.; Colard, C. Presence of cells and fibers immunoreactive toward antibodies to different peptides or amine in the digestive tract of the snail *Helix aspersa*. *J. Morphol.* **1991**, *207*, 185–190. [CrossRef]
59. Franchini, A.; Rebecchi, B.; Fantin, A.M. Immunocytochemical detection of endocrine cells in the gut of *Viviparus ater* (Mollusca, Gastropoda). *Eur. J. Histochem.* **1994**, *38*, 237–244. [CrossRef] [PubMed]
60. Cherif-Feildel, M.; Heude Berthelin, C.; Adeline, B.; Rivière, G.; Favrel, P.; Kellner, K. Molecular evolution and functional characterisation of insulin related peptides in molluscs: Contributions of *Crassostrea gigas* genomic and transcriptomic-wide screening. *Gen. Comp. Endocrinol.* **2019**, *271*, 15–29. [CrossRef] [PubMed]
61. Alba, Y.; Villaro, A.C.; Sesma, P.; Vázquez, J.J.; Abaurrea, A. Gut endocrine cells in the snail *Helix aspersa*. *Gen. Comp. Endocrinol.* **1988**, *70*, 363–373. [CrossRef]
62. Bohórquez, D.V.; Samsa, L.A.; Roholt, A.; Medicetty, S.; Chandra, R.; Liddle, R.A. An enteroendocrine cell-enteric glia connection revealed by 3D electron microscopy. *PLoS ONE* **2014**, *9*, e89881. [CrossRef] [PubMed]
63. Bohórquez, D.V.; Shahid, R.A.; Erdmann, A.; Kreger, A.M.; Wang, Y.; Calakos, N.; Wang, F.; Liddle, R.A. Neuroepithelial circuit formed by innervation of sensory enteroendocrine cells. *J. Clin. Investig.* **2015**, *125*, 782–786. [CrossRef] [PubMed]